

Prestack seismic analysis of the Rangeland Basal Belly River gas pool, Alberta

Ronald Weir, D. Lawton, L Lines

ABSTRACT

The Basal Belly River is a member of the Belly River Formation (BBR), and is the lowermost member, deposited as a marine or tidal sequence. It is a known oil and gas producer throughout Alberta. In the Rangeland area, the Basal Belly River is at a depth of 725 meters, and has a pay thickness of up to 7 meters. Seismic analysis was performed by using forward modeling, and comparing it to actual seismic data. Poststack, and pre stack seismic models were generated, based on the parameters of the 2-D data, and petrophysical parameters derived from well logs. The seismic data was reprocessed, correlated and interpreted using conventional methods. The results indicate the Basal Belly River gas play is a viable seismic target. The Basal Belly River pool in Southern Alberta is Upper Cretaceous in age. It is an exploration and development target using pre stack data analysis.

INTRODUCTION

The Basal Belly River formation is an oil and gas producing formation in Alberta. This formation has been drilled as significant gas and oil target in much of Alberta. The BBR also being evaluated for its suitability in carbon capture and sequestering. The depth and lithology make the Basal Belly River a target suitable for seismic mapping in the Rangeland project area, the BBR has pay thickness ranging from one to seven meters, with porosity ranging from 12 to 21 %, at a depth of 725 meters.

Producing wells in the project area were evaluated for BBR gas pay. There were well logs, historical production data, and perforation intervals used in this report. Petrophysical parameters were determined using the response of producing BBR gas wells. The geological mapping used well logs, production data, and perforation intervals to evaluate the Basal Belly River. Petrophysical parameters were estimated from the well log data base. Gas pay was evaluated primarily using density neutron, and resistivity logs. Perforation information and production data were also used.

The Basal Belly River has been extensively mapped in Alberta using seismic methods. There were a number of 2-D seismic lines available in Twp. 38 R 20 W4 to interpret and evaluate. Three seismic lines were selected that tie existing BBR production. In this project Pre and poststack inversions were generated to evaluate the suitability of the method for Basal Belly River Hydrocarbon detection. The results of the seismic methods were compared to the geological mapping

In the Rangeland area, the amplitude versus offset analysis was used for direct gas detection in the Basal Belly River formation in Southern Alberta. 2-D seismic reflection data was interpreted and analysed to determine the seismic response of a gas charged reservoir. The seismic data was selected because it was positioned across a known, existing producing belly river pool. Three seismic lines were reprocessed in

an amplitude versus offset compliant flow. The data were inverted both pre and poststack. Displays were generated of gathers, super gathers, stack, inversions. The results of the forward modeling, and inversion were compared with the well data. Recommendations were made as to the suitability of these seismic techniques using vintage seismic data for BBR evaluation.

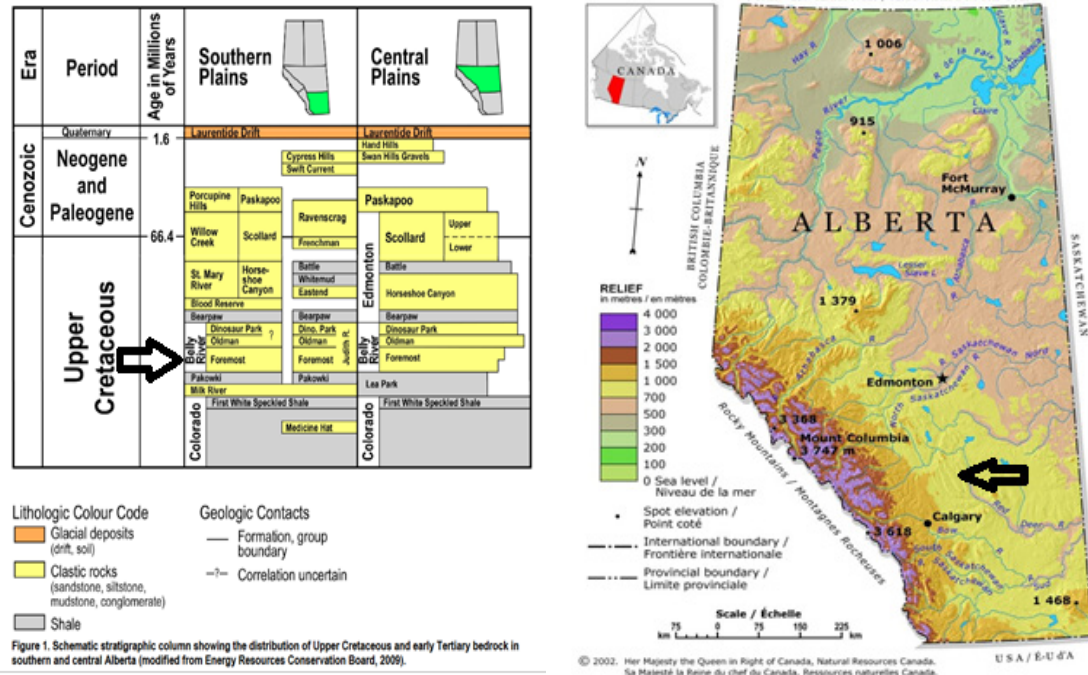


FIG. 1. Project area and South and Central Stratigraphic Chart. The arrows illustrate the target formation, and the geographical area of the Rangeland project. (Courtesy ERCB and Natural Resources Canada).

Forward modeling was performed using an existing dipole sonic log at 03-18-38-20W4. Estimates of petrophysical rock properties were derived from well log data over the producing BBR pool at 04-12-34-22W4. The forward modeling was matched to the acquisition and wave forms of the actual data.

Seismic data were provided by Pulse Seismic as part of their proprietary data base. This consisted of two 1980s vintage 2-D seismic lines, and one 2002 vintage line. These lines were reprocessed to be amplitude vs. offset compliant, and interpreted. Displays were made of stacks, gathers and super gathers. Seismic inversions were processed, both post and prestack datasets. The results of the seismic data analysis were compared to well logs and production data. The suitability of amplitude analysis, inversion (pre and poststack) show that Gas pools can be evaluated acquired over the Rangeland pool exists and three 2-D reflection seismic lines were analyzed.

A forward looking strategy was presented for the use of vintage seismic data for BBR exploration and production. Recommendations were made for future strategies using vintage data. Future data acquisition to evaluate the Basal Belly River are also discussed.

GEOLOGICAL MAPPING

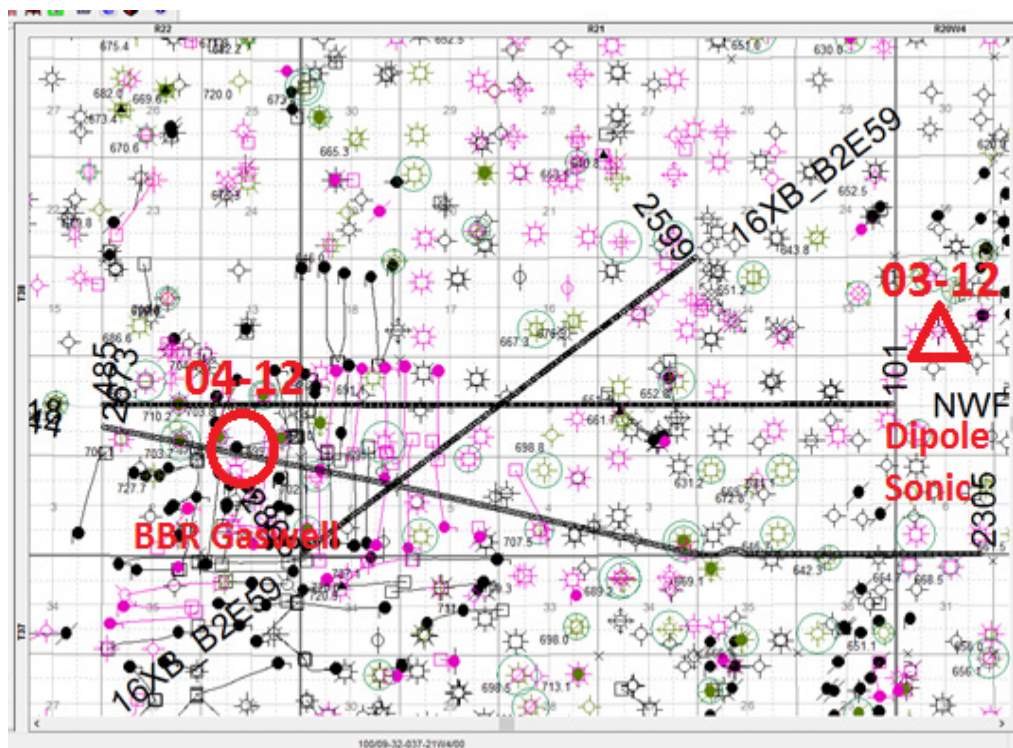


FIG. 2. Area Map showing well and seismic control. This map shows the well control, the seismic lines, and the key dipole well location used for modeling. Many of the wells shown are deeper targets, or wells completed in the mid to upper Belly River.

Area Geology

The Basal Belly River (BBR) is the lowermost facies of the Cretaceous Belly River formation. The primary production is gas, with some oil production in Western Alberta. It is comprised primarily of fine grained sandstones, with some coarse grained beds, coal, green shale, and concretionary beds. There is some bentonite present, making the producing zones subject to drilling damage. There are local occurrences of thin, localised coarse grained sand (Alberta Geological Survey 2016)

The Basal Belly River is rich in bentonite, a swelling clay mineral. It is highly susceptible to drilling damage, especially if it is exposed to fresh drilling mud over a long period of time, if it is drilled as a primary target, there are minimal issues with damage. Frequently, the BBR is treated as a secondary target for a deep well, and is exposed to fresh water drilling mud for extended periods of time. Perforation intervals can be indicative of pay; frequently the BBR was perforated as a secondary objective in conjunction with several other pay zones. This is why it is difficult to produce an isolated production map of the BBR.

A producing Basal Belly River well is located at 04-12-38-22W4. The gas pay is in two zones, at a depth of approximately 725 meters (See Appendix 1). The gas pay can be seen by examining the crossover of the density and neutron log curves (Crain 2000). The producing sand varies in porosity from 12 to 21 %. The gamma ray indicates that

there is a high shale content in this sand. The well at 04-12-38-22W4 is used for forward modeling to compare the response of a gas filled sand reservoir, to a non-producing regional well located at 04-18-38-20W4. The intent of the forward modeling was to simulate actual reservoir conditions as accurately as possible. Actual well logs were used, and gas pay zone logs were inserted to simulate the zero offset seismic response.

The rangeland area Basal Belly River deposition is estuarine tidal dominated (Boulder Operations 2016). Log signatures in this area show coarsening upward, fining upward, and blocky sand. The distribution of the clean reservoir quality sand is difficult to predict based on well log data and trend mapping alone. Unlike offshore barrier bars, marine channels, estuarine channels may have seemingly random occurrence. The broad channel systems can be mapped, but the specific occurrences of reservoir quality sand are difficult to predict without seismic

Estuarine depositional environments are subject to rapid changes in river flow, storm surges, tides, and variations in sediment. Estuaries such as the Han River in Korea can deposit and remove several meters of sediment in a short period of time (Chung 1990, Choi et al, 2006). The estuary displayed in figure 3 is of the same general scale as the BBR feature mapped in rangeland.



FIG 3. Estuary Example, Scotland, River Nith. This is a modern day template for the Basal Belly River. Imagine this estuary being preserved by a marine transgression. Estuaries will deposit, erode, and resort sediments due to seasonal changes in flow, storm surges, changes in sediment load, and tidal fluctuations (such as the Han River in Korea).

In the river Nith example shown in figure 3, the estuary system is wide, the specific sand bars are quite localized. If one were to imagine a marine transgression as shown in figure 3, the entire system would migrate inland, and the sand and channels would be preserved. The contoured sand trend (figure 6) was interpreted to be in a predominantly North-South alignment as proposed by Irwin (1980).

A geological cross section was constructed using Geoscout. The cross section contains two regional BBR wells at either end, with two producing BBR wells in the middle. The two producing wells had 7 and 3 meters pay. The Base of the BBR was used for a geologic datum. The 04-12 well shows density neutron cross over, and two perforation intervals (figure 5 and appendix 1). The gamma response was somewhat muted, the BBR sand has a high clay and mineral content.

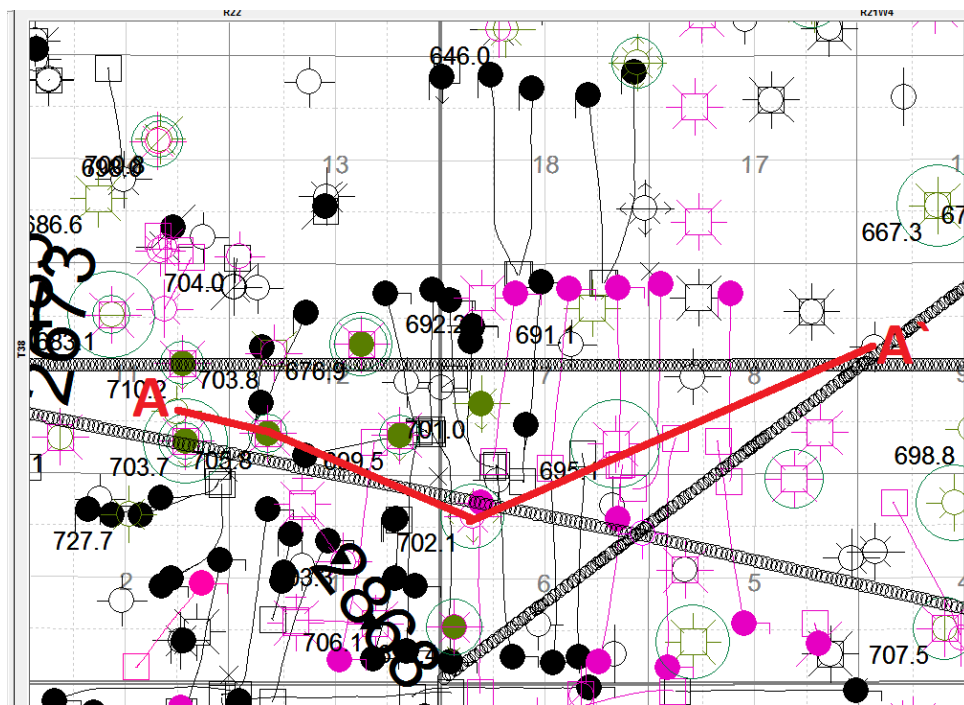


FIG 4. Geological Cross Section reference map. The highlighted section in red ties two BBR gas wells, and two tight wells. The pool is assumed to run approximately North-South.

A contour map was created using 2 meter pay intervals in the BBR. The porosity cut off was 12 %, with porosities as high as 21 % at the 04-12 location figure 06). Many of the locations were not deep enough, no logs, or old logs. The contours were influenced by the seismic amplitudes; strong seismic BBR amplitudes were equated with BBR gas pay. This was a subjective trend interpretation that tied wells with pay to strong seismic amplitudes.

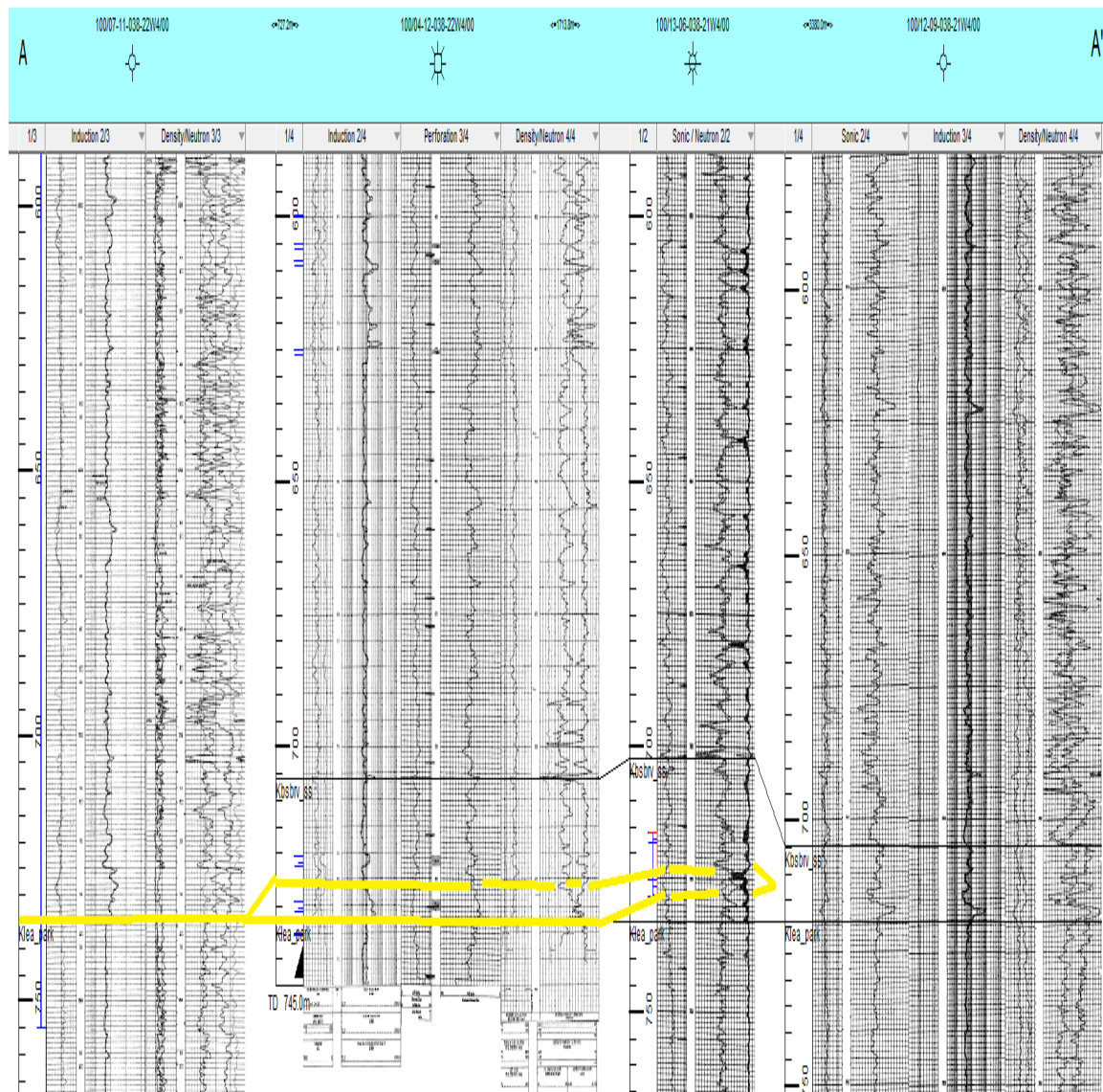


FIG 5. Geological cross section. This cross section was chosen to illustrate the nature of the Basal Belly River deposition. The cross section includes tight, non reservoir facies, and porous gas filled channel. This cross section goes from non reservoir (07-11), to 7 m pay (04-12), 3 meter pay (13-06) to non reservoir (12-09). The sand facies are highlighted in yellow. A larger version of this cross section is included in Appendix 1 of this report. (see figure 7 for detailed log on the 04-12 location)

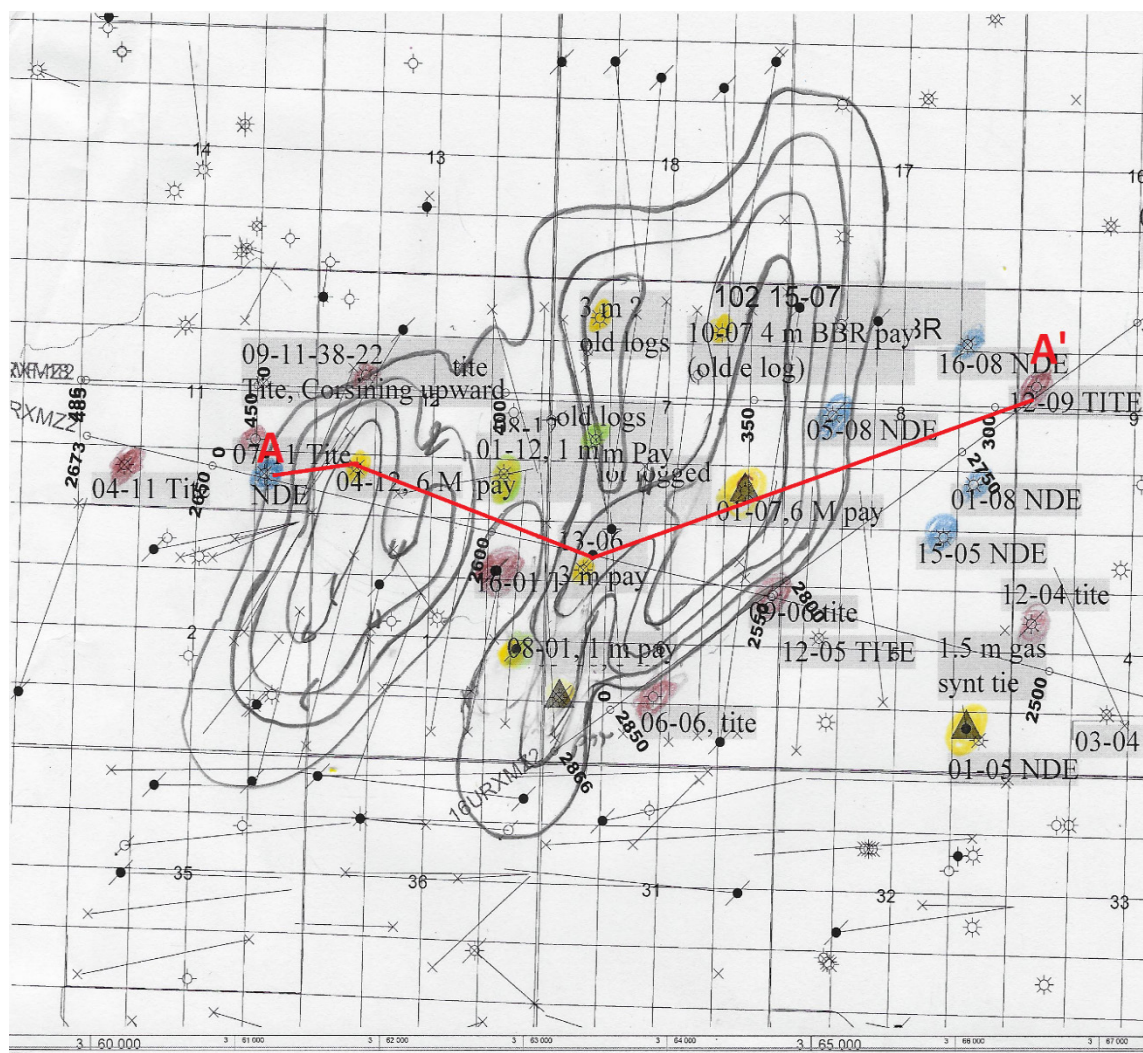


FIG 6. Base Belly River, Net Pay, Pay Zone. This shows the wells used in the geologic interpretation of this area. The porosity cut off was 12 %, The contours took into consideration the seismic amplitudes. The contours were influenced by the seismic amplitude map, and are in 2 meter increments. Perforation intervals were used in conjunction with log data.

Yellow: Pay > 3 M.
 Green: Pay 1 – 3 M.
 Brown: Tight or < 1 M
 Blue: Not deep enough, no logs, or old logs

SYNTHETIC SEISMOGRAM GENERATION

A synthetic seismogram requires a sonic log, or a sonic plus density log. The sonic log is used to convert depth to time, and the density with the sonic create the zero offset reflectivity. This reflection series is convolved with a wavelet to generate a synthetic seismogram. The bandwidth of the wavelet is estimated based on the bandwidth of

seismic data to be tied. A more accurate synthetic is calculated when both sonic and density logs are available. In this study, there were no sonic logs available over the gas pool. A density log at the 03-18-38-20W4 location was used to calculate the sonic log as defined by Gardner's Equation (Crain, Ross, 2000)

The well at 04-18-38-20W4 has a full set of logs, including a dipole sonic. The Basal Belly River well at 04-12-38-22W4 had only density and resistivity logs available.

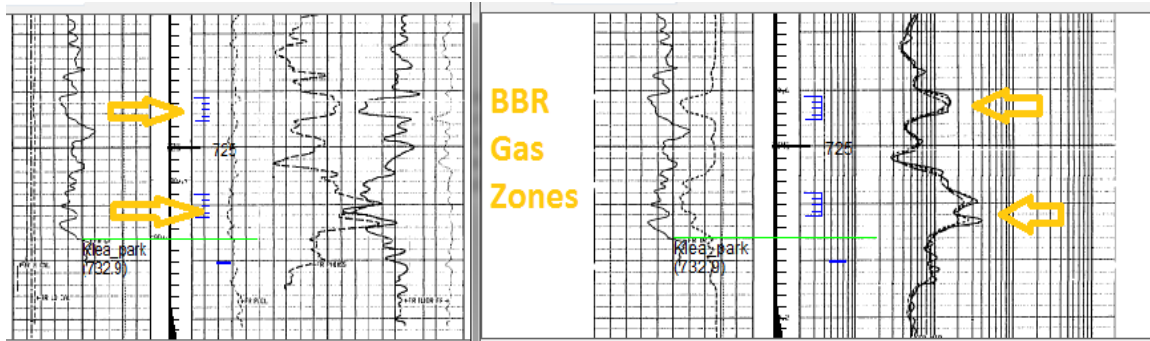


FIG 7. Gas Pay Zones The logs at 04-12-38-22W4 are shown here. The density and induction logs highlight the two pay zones. These are used to model the zero offset response. This well produced gas from the BBR, the perforation zones are shown. Gas was produced from the two zones as indicated; gas is shown on logs of high resistivity, and the convergence of the density and neutron porosity. Maximum porosity was 22 %

Gardner's equation was used to estimate the velocity from the density in the gas pay zones. Gardner's equation is: $Velocity = .3048 \left(\frac{density}{229.5} \right)^4$

The parameters .3048 and 229.5 are area dependant. The velocities derived from the density in this case were, on average, faster than the actual sonic in 04-18-38-20W4. To compensate for this, the relative changes are used, not the absolute values. Errors in conversion from density to sonic occur if logs are not properly calibrated. For this modeling, actual pay thickness was used, Gardner's equation is used to estimate contrasts in p-wave velocity over a well in the BBR pool. The calculated values for the sonic log were inserted into the log suite at 03-18 to simulate gas pay.

To simulate gas, the sonic log velocity from 04-18 is reduced by 1000 meters per second, the density reduced by 220 Kg per cubic meter. These values are used to block the original sonic and density logs from the 04-12-38-20W4 location. (This adjustment is consistent with the calculation from Gardner's Equation). This simulates the conditions for free gas zones in the Basal Belly River.

To construct a model, the first step is to generate a zero offset synthetic seismogram. This is calculated using the 04-18 sonic and density log. A second seismogram is calculated using the same logs, but with the sonic and density values modified to match the 04-12 BBR gas well. These two logs are loaded into the modeling program and

placed 1000 meters apart on a modeling grid. The model is constrained to interpolate sample by sample from the original log, to the well simulating gas response. The interpolation is constrained between the top and base of the Basal Belly River.

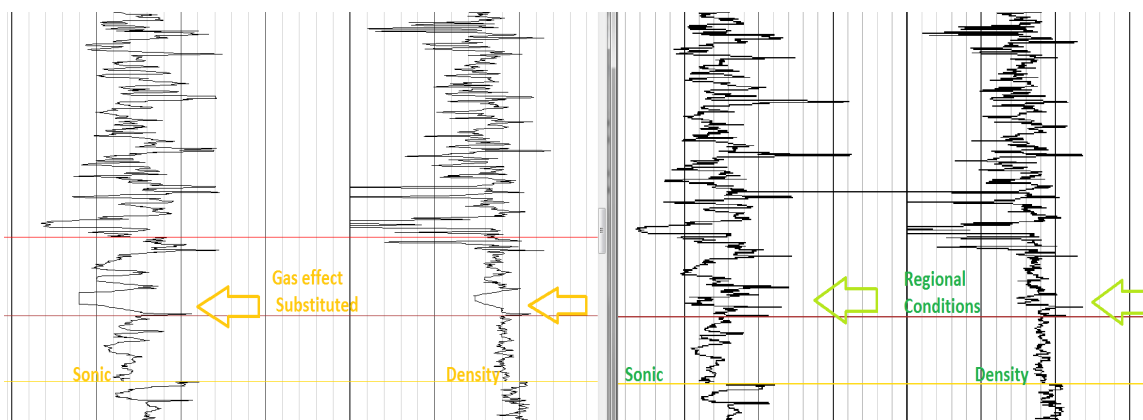


FIG 8. Model Input Log. This figure shows the regional and the model logs going from gas (left) to regional (right). The target zone is highlighted with arrows. To simulate gas, the sonic and density are blocked as shown.

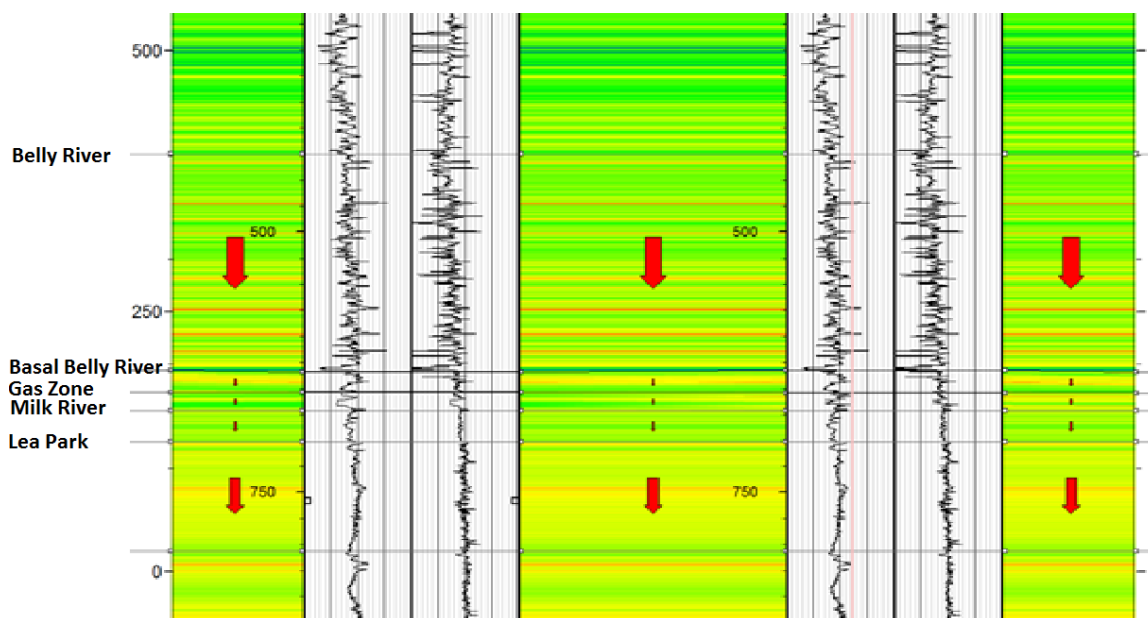


FIG 9. The Zero Offset Forward Model. The calculation of the model involves interpolation of the impedance between the two locations. Here there is the original log (right), and the inserted porosity from the 04-12 Location (Right). A wavelet is convolved with this reflection coefficient series and produces the synthetic seismogram in the next figure. For this model, all geological intervals remained constant, changes of thickness were not taken into account.

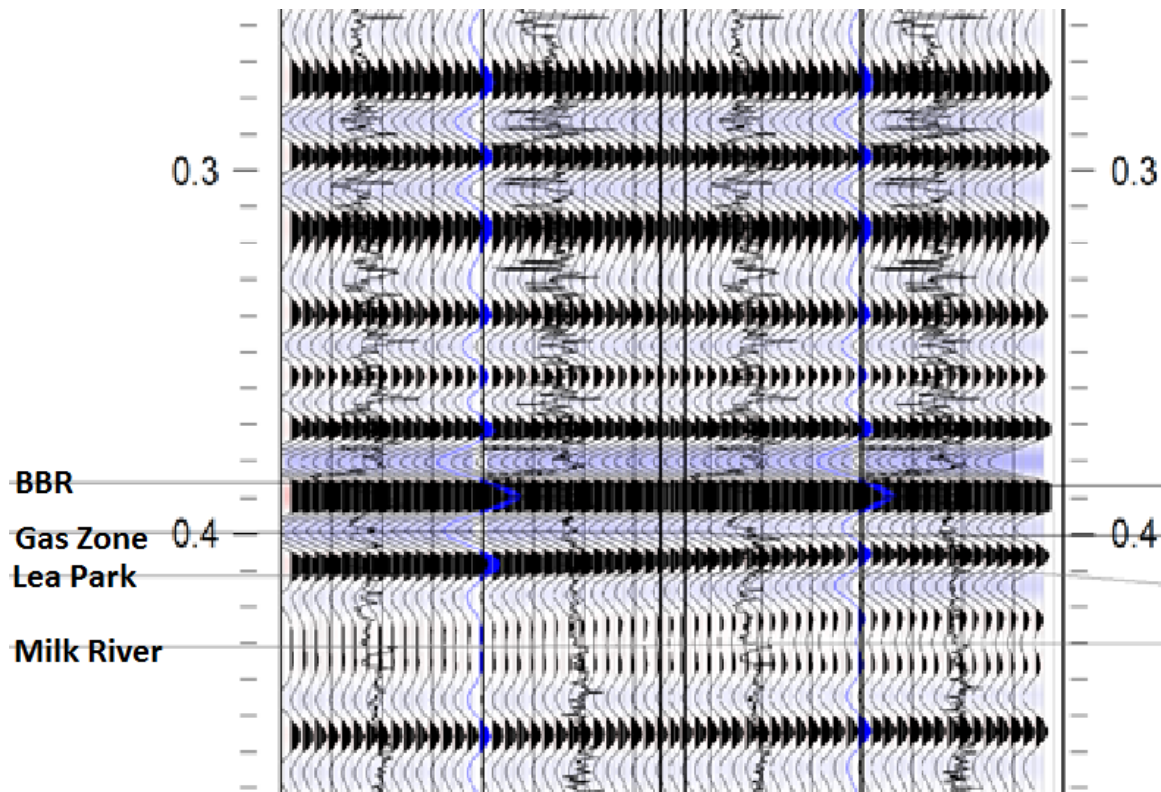


FIG 10. Zero Offset Seismic Forward Model. The wells are located at the blue trace in figure 5. Seismic responses between, and outside the well ties are interpolated. This shows the range of responses from the left blue trace, (full gas pay) to the right blue trace (regional). The amplitude shows a marked increase when the gas effect is inserted. There is also an apparent dip and thickening of the structure, due to the changing reflection coefficients. The wavelet is a zero phase Ormsby 08-12-60-70.

The forward modeling suggests that this type of facies changes and gas saturations are observable in zero offset reflection seismic data. The wavelet used for this model is a visual estimate of what is actually in the data. The model shows the base of the Belly River Gas zone appears to drop in structure. This is not the case, in that the major reflection occurs at the base of the gas pay zone and gives the *appearance* of a structural low, or “channel.” The input model does not have any structural changes from the gas model to the regional. What is being shown is the combined reflection response from the base of the gas zone.

This model suggests that reservoir mapping and seismic interpretation in the Basal Belly River involves the identification of these *apparent* structural lows. This will change when the wavelet used is extracted from the actual data. the bandwidth of the actual seismic data.

Isaac and Lawton in the 2016 GeoConvention presented a Basal Belly River modeling study that demonstrated that zero offset synthetics do not tie well over the BBR interval. When the non – zero angle components were included the synthetic match to actual data was very good. According to the 2016 presentation, modeling

using an s -wave, p-wave and density produced a much better match to the stacked seismic data. Data from the higher offset angles made a significant contributor to the CMP stack.

AVO FORWARD MODELING

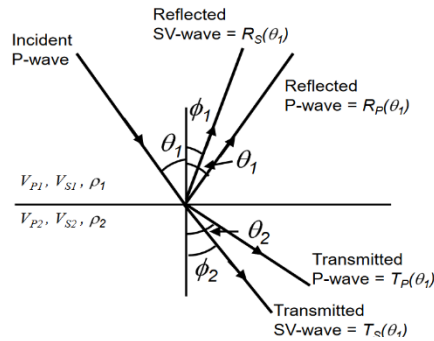
Theory

The forward modeling described in the first section (ZOS) does not take into account reflectivity that occur at a non-zero incidence. The models generated in the AVO section take into account the way in which the acquisition geometry, the data extracted wavelet, and the non-zero nature of the seismic reflection.

Mode Conversion of an incident P-Wave

HAMPSON-RUSSELL
A Geophysical Company

More technically speaking, if $\theta > 0$, an incident P-wave will produce both P and SV reflected and transmitted waves. This is called *mode conversion*.



10

The Aki-Richards equation

HAMPSON-RUSSELL
A Geophysical Company

- Any other angle is modelled with the Aki-Richards equation, a linearized form of the Zoeppritz equations which is written (and is the basis of virtually all AVO methods):

$$R(\theta) = aR_{VP} + bR_{VS} + cR_D,$$

$$\text{where : } R_{VP} = \frac{\Delta V_P}{2\bar{V}_P}, R_{VS} = \frac{\Delta V_S}{2\bar{V}_S}, R_D = \frac{\Delta \rho}{2\bar{\rho}},$$

$$a = 1 + \tan^2 \theta, b = -8K \sin^2 \theta, c = 1 - 4K \sin^2 \theta, \text{ and } K = \left(\frac{\bar{V}_S}{\bar{V}_P} \right)^2.$$

- The Aki-Richards equation says that the reflectivity at angle θ is the weighted sum of the V_P , V_S and density reflectivities.

FIG 11: General Non Zero incident reflection description and the Aki-Richards equation (from the Hampson Russell course notes).

AVO Curves

HAMPSON-RUSSELL
A CDVortex Company

This figure on the right shows AVO curves computed using the Zoeppritz equations and the Aki-Richards equation for the top and base of a gas sand model.

Notice that the fit is quite good in this case.

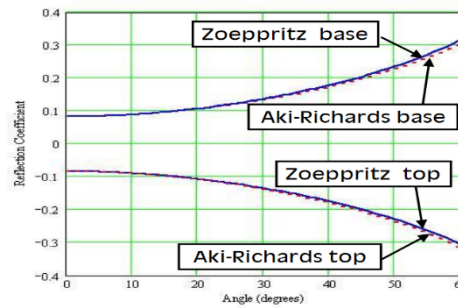


FIG 12. General Class “C” Gas Sand Showing the reflection coefficient as a function of offset. (from the Hampson Russell course notes). Note that the offset model shown here goes to 60 degrees. Line 14 had useable data to 30 degrees.

The AVO synthetic was designed to image the Basal Belly river using actual geological parameters. The gas sand, is acoustically slower than the shale above and below it, making it a class “A” sand. This means that the reflection coefficients at the top and base of the sand will increase as a function of offset.

In order to generate an accurate offset dependant model, parameters from 04-12-38-22W4 were inserted into the 03-18 log. This was the same exercise as performed in the zero offset synthetic model. To simulate the shear wave response, a first guess was made by selecting V_s from the lower 2ws sand. This was again edited to ensure the Poisson ratio remained positive, and within reasonable parameters for gas sand (*1.0 to 1.8 in this case*). These two synthetics represent the two extremes one expects to see in this area. Seven meters of gas pay, compared with tight regional sand.

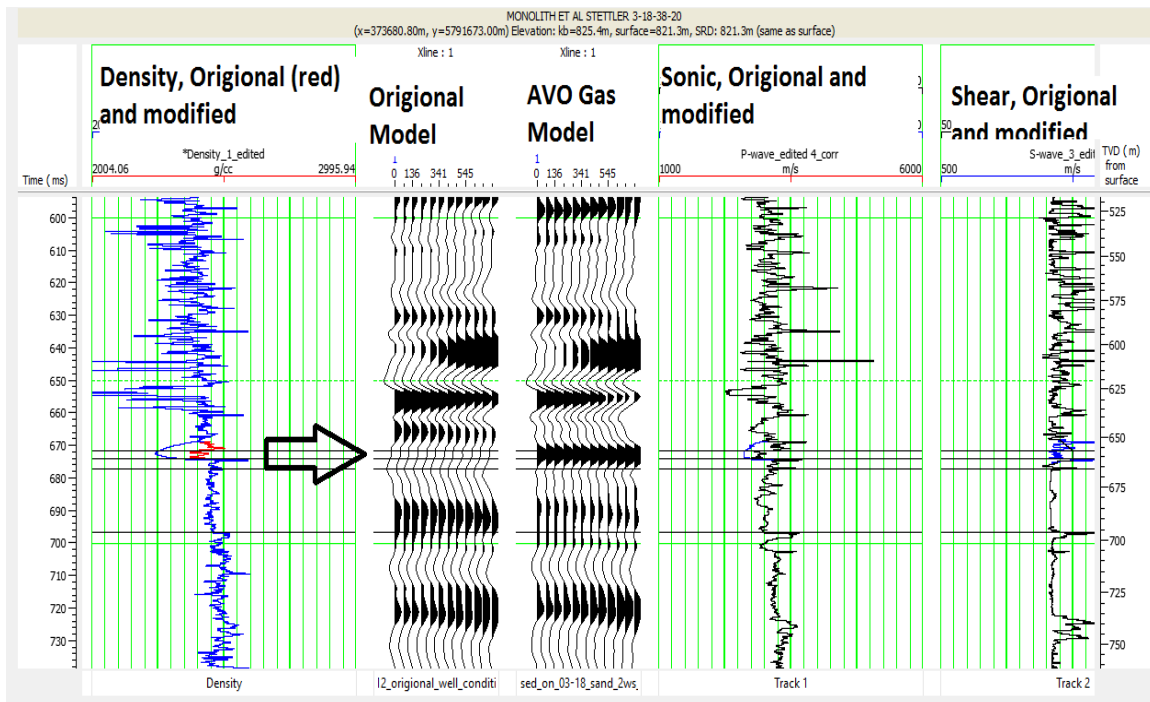


FIG 13. AVO Seismic Forward Model. This AVO forward model shows the unmodified log, and the modified logs simulating gas parameters. These conditions represent the maximum and minimum gas pay expected in this area, compared with the zero pay regional deposition. The maximum offset is 700 meters, or 30 degrees. This matches the useable range of offsets in the seismic data. The log parameters were derived from the 04-12 BBR gas well. The model shows an increase in AVO when gas is present. The sonic density and shear wave curves are shown. The curves are shown as the original logs and the modified logs. The V_p/V_s ratio is constrained to a minimum value of 1.42.

An offset dependant forward model is created from a dipole log going through a BBR gas zone. In this case there was no direct measurement of a shear wave velocity over any producing BBR sand reservoir in this area. Estimates were made using the lower Second White Specs (2WS) sand, and zones from the middle Belly River. as a guideline. The S wave velocities are again edited to ensure the Poisson ration stays within a reasonable range for gas sand of 1.0 to 1.8. Gas saturation has a relatively small affect on shear wave velocity, but a large negative acoustic affect on p-wave and density. For the class C sand modeled here, the p-wave reflectivity increases as a function of amplitude with offset.

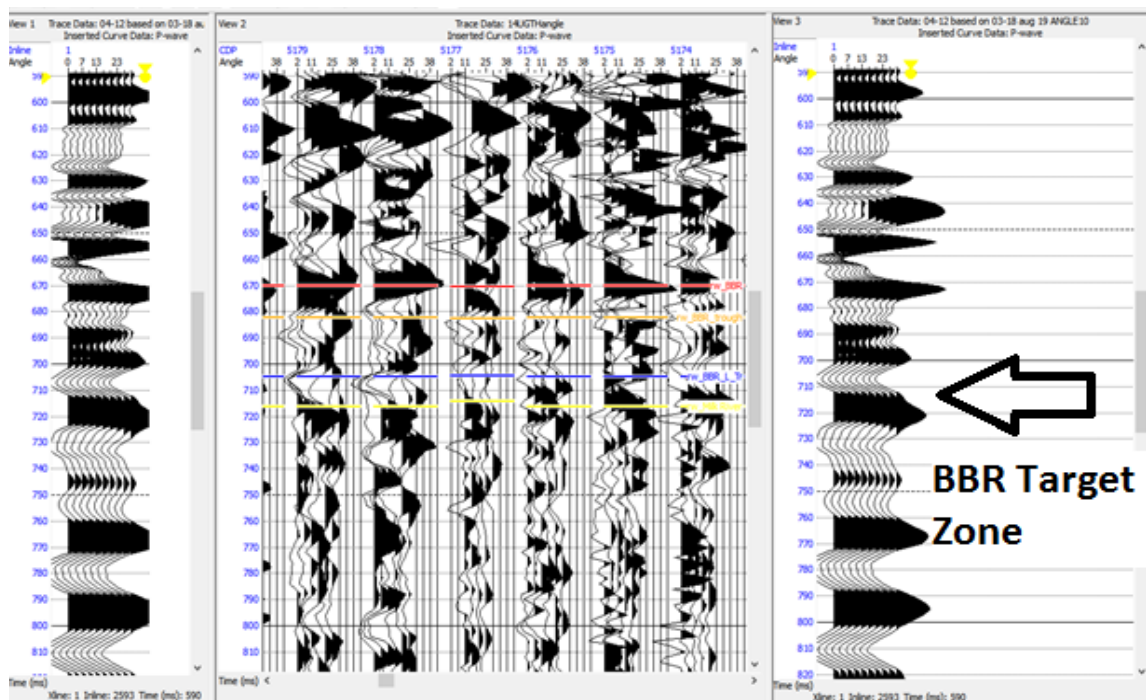


FIG 14. AVO forward gas model with CDP gathers. The seismic data model was matched to the valid seismic data to ensure the modeled range of offsets matched the useful seismic data. Both data and model displays are from 0 to 30 degrees. The wavelet used from the model was extracted from the seismic data over the zone of interest.

Forward Modeling Summary and Predictions

Based on the forward modeling, Basal Belly River AVO effect is observable on seismic data. The wavelets used for modeling were extracted from the actual seismic lines. The AVO forward model was based on the best BBR well in the area. The conventional stack was predicted to show a strong amplitude anomaly at the target zone, consisting of a strong trough / peak combination. The AVO forward modeling predicted a strong increase in amplitude with offset, based on the best well in the area. Offsets were limited to 30 degrees, to match the seismic data. This situation is often called a class C amplitude effect. The P-wave velocity is slower than the formations above and below, causing a bright spot on the stack sections.

Under ideal conditions The pre stack inversion, would show a low P-wave impedance, a low V_p / V_s ratio, and a low density impedance. The poststack inversion was predicted to show a low impedance zone in the proximity of the well. The gas was predicted to be directly observable on CMP gathers and super gathers.

The analysis of the data would show additional area suitable for BBR exploration. The model based pre stack inversion is predicted to identify gas effects such as V_p/V_s , Z_s , and Z_p . The equations in figure 11 are used for forward modeling and the pre stack elastic inversion. (FIG 24 and 25)

Seismic Data

Three seismic lines were acquired from Pulse Seismic *. These were:

-16XBB_B2E59	February 1982,	1200% Vibroseis	(Line 16)
-NWF-18	June 2005	1200% Dynamite	(Line 18)
-14Y_A4M44	September 1980	1200% Dynamite	(Line 14)

These three seismic lines were acquired over the mapped BBR pool, lines 14, 16 and 18. These lines were licenced to the University of Calgary. The lines were originally shot for Mississippian and Devonian targets. Line 14 was selected for detailed analysis, it had a good range of offsets and reasonable data quality. It also tied a number of BBR wells, both tight and gas sand.

**These seismic lines were acquired under license from Pulse seismic. If this information is to be published outside of the University of Calgary, permission must be obtained from pulse. Pulse may require the specific locations of the lines be removed*

DATA PROCESSING

The seismic line was reprocessed at Statcom in an AVO compliant manner. Care was taken to preserve AVO effects. In particular, the mute was designed to let in as much offset data as was reasonable. The stacked version of this same data was used for interpretation and pre stack inversion. The gathers used were NNO corrected, and were input for the first prestack inversion process; and F-X prediction was run on the gathers for a comparison.

Surface consistent scaling was used to reduce source to source and geophone amplitude fluctuations due to source strength, geophone coupling, surface conditions, and noise. The instantaneous amplitude for each input trace was calculated over a specified window from 250-2200 ms. at 75 m of offset and 950-2300 ms. at 1845 m of offset for this data. The instantaneous amplitude was then decomposed into source and receiver terms in a best-fit sense by using the Gauss-Seidel algorithm. Traces that fall outside a specified DB range around the reference mean are automatically edited. The reference amplitude chosen for scaling purposes was 2500.

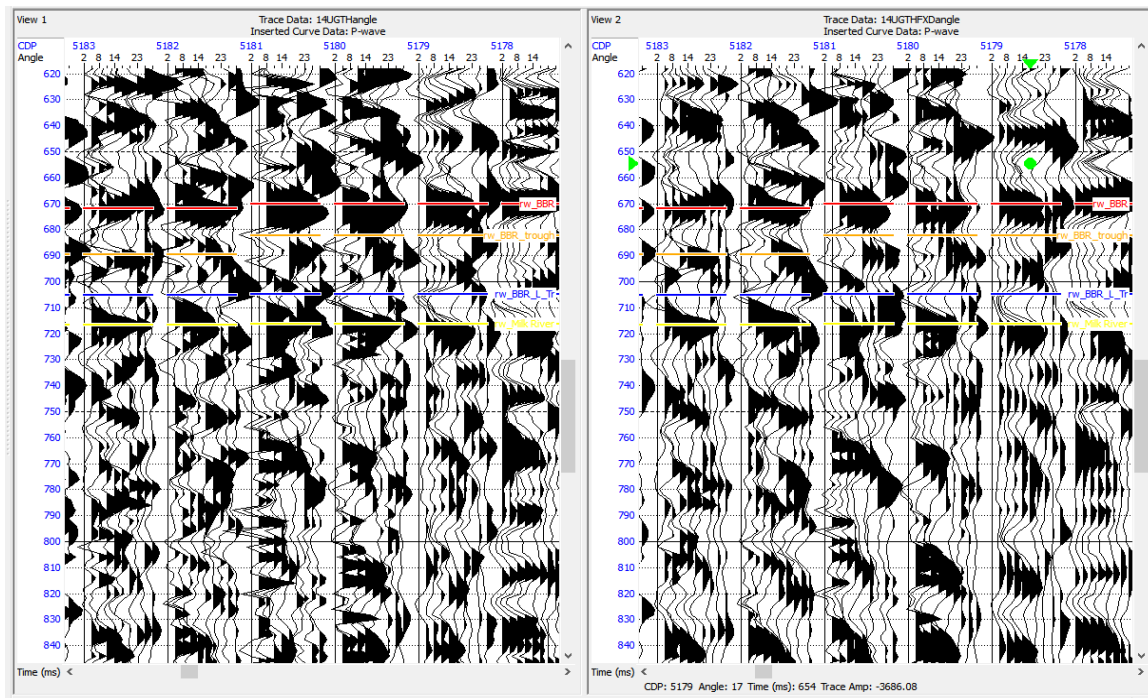


FIG 15. The effect of the F-X Deconvolution-X deconvolution was run using Vista. There was a significant reduction in random noise.

Line 14 had a useful offset at the 700-meter belly river target of 700 meters. Based on the time to depth curve this equated to an incident angle of 30 degrees. The useable range of data at this depth was 6 fold. The gathers were resorted for interpretation and inversion into common angle gathers

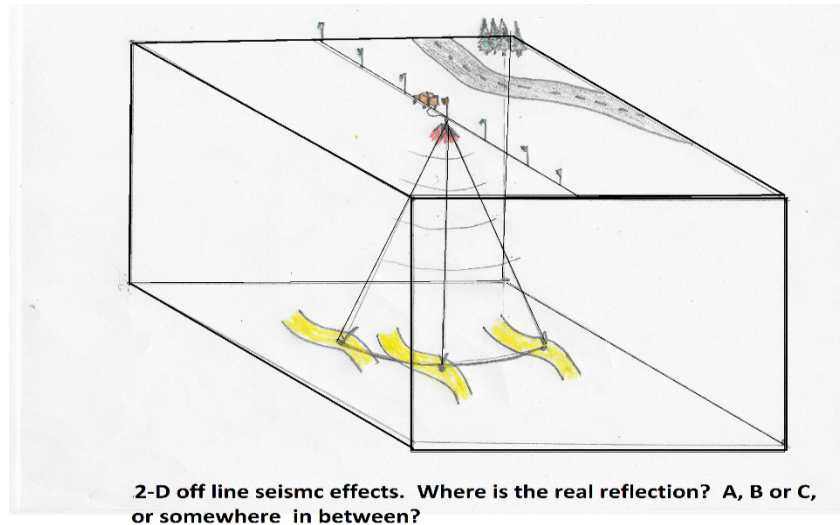


FIG 16. A Fresnel Zone Illustration. Where is the actual seismic reflection event? With 2-D data there is no unique solution for off line effects.

CONVENTIONAL SEISMIC INTERPRETATION

The data were reprocessed and the stacked section was relatively noise free. Five conventional seismograms were generated in the area at different locations, and incorporated into the Seisware® project. Two of the synthetics were generated from deep Devonian wells, enabling the correlation and depth matching to be quite accurate. Correlations were made for the top Belly River, Top Basal Belly River sand, Milk River, and Manville. The synthetic ties were very good, down to the deepest correlation in the Precambrian. Two additional picks were made on troughs internal to the BBR unit with the intent of tracing seismic amplitudes. These correlations were later used to constrain the inversion and produce the initial pre and poststack inversion models.

The forward modeling indicated an amplitude response in the BBR zone when gas is present. A seismic amplitude map should resemble a gas pool map in general terms. High amplitude events were noted, and investigated further. The limitation inherent in amplitude interpretation is that many different geological changes can induce strong amplitude effects. These include coals, tight high impedance sand, and tuning effects. The forward modeling did not include such things as pinch out, juxtaposed stratigraphic layers and so on. The geological mapping in this area indicated that wet BBR sands were not expected in this area.

As far as the general trend mapped on the seismic data, there is a good correlation between the mapped amplitude effects on the seismic data, and the Basal Belly River gas pool. Figure 17 combines the 2 meter BBR gas pay cut-off with the seismic amplitude. The general trends line up quite well, there is an amplitude mistie at the intersection of lines 14 and 16, indicating that there may be some off line effects at the BBR zone. A concern with 2-D data was off line, Fresnel zone effects. Line 14 and line 16 tie the 09-06-34-21 location. Well logs indicate the sand is tight at this location. The amplitude response for line 14 and 16 differ in amplitudes at 09-06, suggesting there may be a gas reservoir nearby, but out of the plane of the section

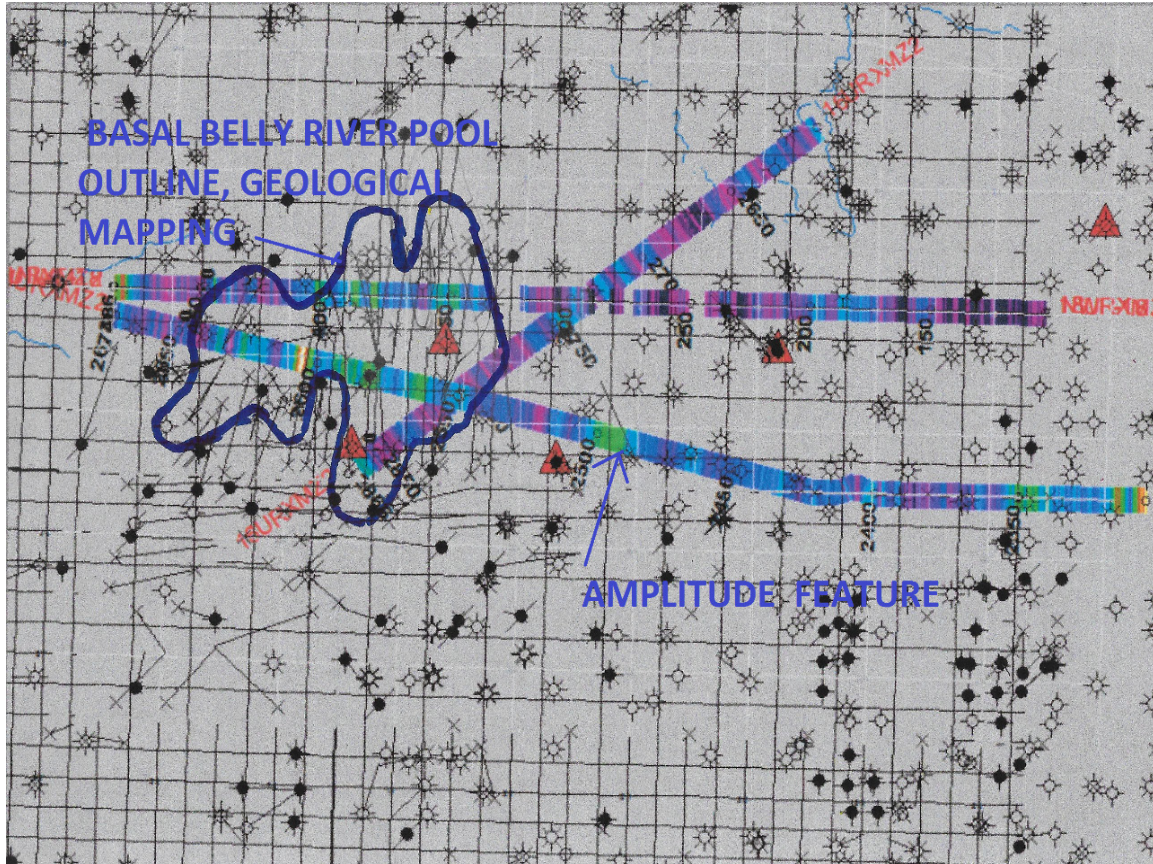


FIG 17. A comparison of seismic amplitude to the pool boundary. The Basal Belly River pool outline is shown in blue, The seismic amplitudes in colour. There is a reasonable match between the colour seismic and the pool outline. There is an undrilled amplitude anomaly at 10-05-34-21. This is also evaluated for AVO response. Line 14 and line 16 intersect at the 09-06 location, and show different amplitude responses. Strong amplitudes are green, weaker amplitudes are purple.

Amplitude maps were produced on the Base of the BBR. The forward modeling predicted that there would be increased amplitude over this zone, and the amplitude map demonstrates this. The amplitudes can be caused by other features, such as coals, tight sands, tuning. The bandwidth of the data has a bearing on the overall seismic response. The forward zero offset model was matched qualitatively to the seismic data

on frequency, assuming zero phase. The amplitude feature shown in figure 17 bears a good general match to the geological mapping for gas pay. There are other significant amplitude features that were investigated outside of the mapped pool boundary.

There is an undrilled amplitude anomaly identified at 07-05-34-21. In an exploration project, this anomaly would warrant further investigation. Amplitudes can also be caused by high velocity sand, coals, or tuning between beds. Prestack inversion and AVO analysis reduce the number of interpretation effects for anomalies. This anomaly is evaluated in the analysis part of this paper.

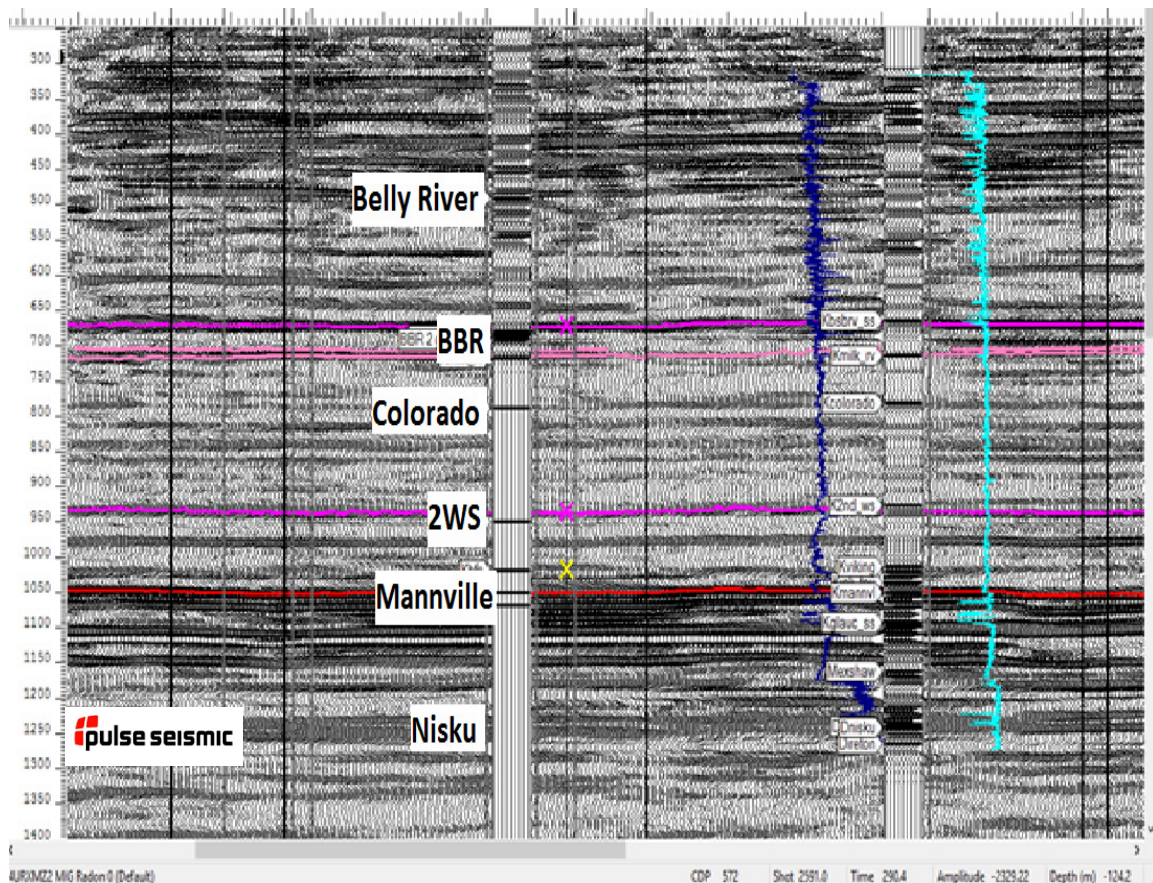


FIG 18. Seismic correlation with well log Zero Offset. The correlation between the seismic data and the zero offset synthetic is shown here. The well tie correlates from the top of the Belly River to the Devonian. All three seismic lines were tied and interpreted. The deep logs were available to tie events as deep as the Devonian. This gave an exact tie to the BBR target zone

POSTSTACK INVERSION

A poststack inversion was carried out on line 14. This adds the 0-15 Hz low frequency component to the data from the p-wave and density logs. This inversion

served the dual purpose of generating the initial model for poststack, and then for prestack inversion. The seismic picks, the extracted wavelet, and the synthetic tie are all the same. The output for the poststack inversion is acoustic impedance, with the colour bar optimized to show impedance contrast in the BBR zone. Seismic events picked on the stacked section, are transferred to the prestack data, and interpolated into the offset domain.

The results of the poststack inversion are seen on figure 19, the low impedance zone matching nicely with the mapped geologic boundaries of the BBR pool. Toward the West end of the line, the data degrades, as does the results from the inversion. The East boundary of the pool is easy to see, the west, less so because of a noisier seismic section. The pool isopach increases from East to West. The west boundary is difficult to spot; noise has become a factor over the 04-12 tie.

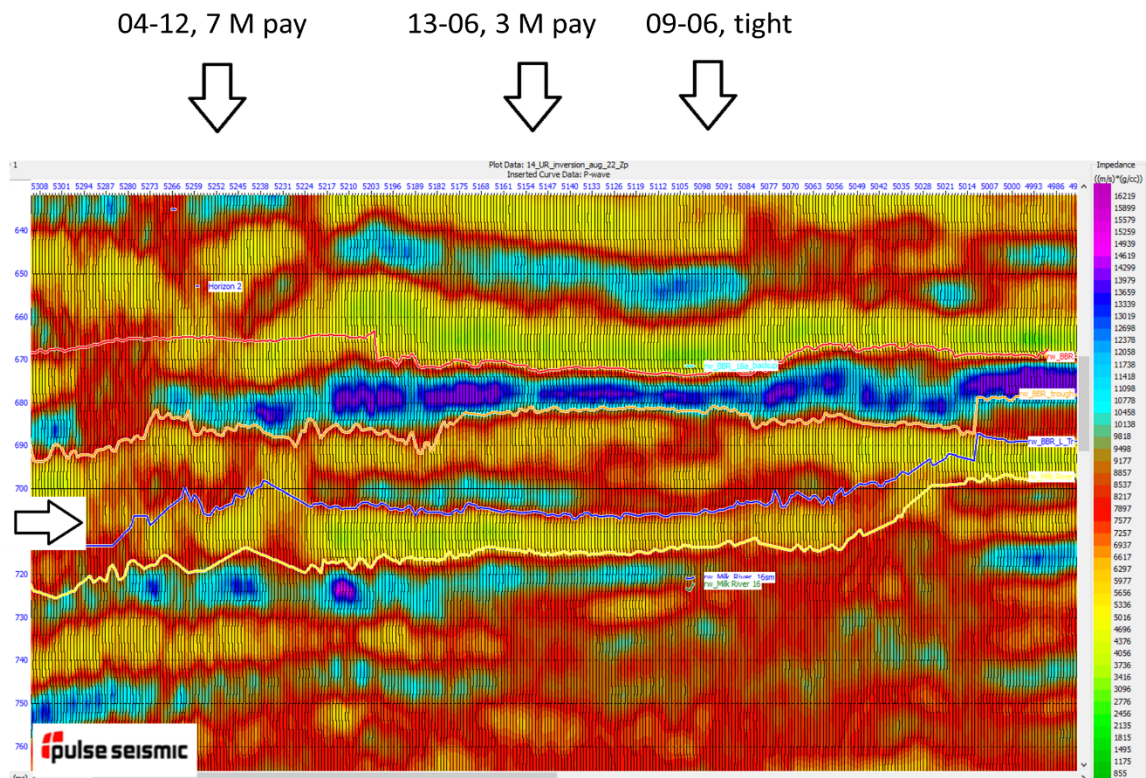


FIG 19, Poststack inversion. The inversion shows the East pool boundary, and a thickening as the pay increases from 3 meters to 7 meters in the West direction. The signal is then lost in the noise, making the inversion difficult to interpret. The inversion generated good results in the vicinity of the 13-16 gas well. The quality of the data deteriorated to the west, making it difficult to map the reservoir. To the West of the 13-06 well, there are indications of low impedance as seen in the transition to yellow on the display. 13-06 is 300 meters North West of the seismic line. It was mapped with 3 meters of gas pay.

AVO ANALYSIS

The data was prepared for AVO analysis by tying the data to a sonic log, creating a time to depth conversion (Figure 20). Angle gathers were calculated from CMP gathers using a sonic from a well tie. In this case, the useable offset was 30°. A plot of the angle gathers and the CMP gathers are shown in figure 21. A line is drawn to show the 30° cut-off at the zone of interest. This gave a fold of 600 % at the Basal Belly River. Data such as the well tie, time-depth curves, seismic event picks, and the extracted wavelet was transferred to the prestack inversion. The seismic event picks were flat line interpolated into the offset domain from the zero offset trace.

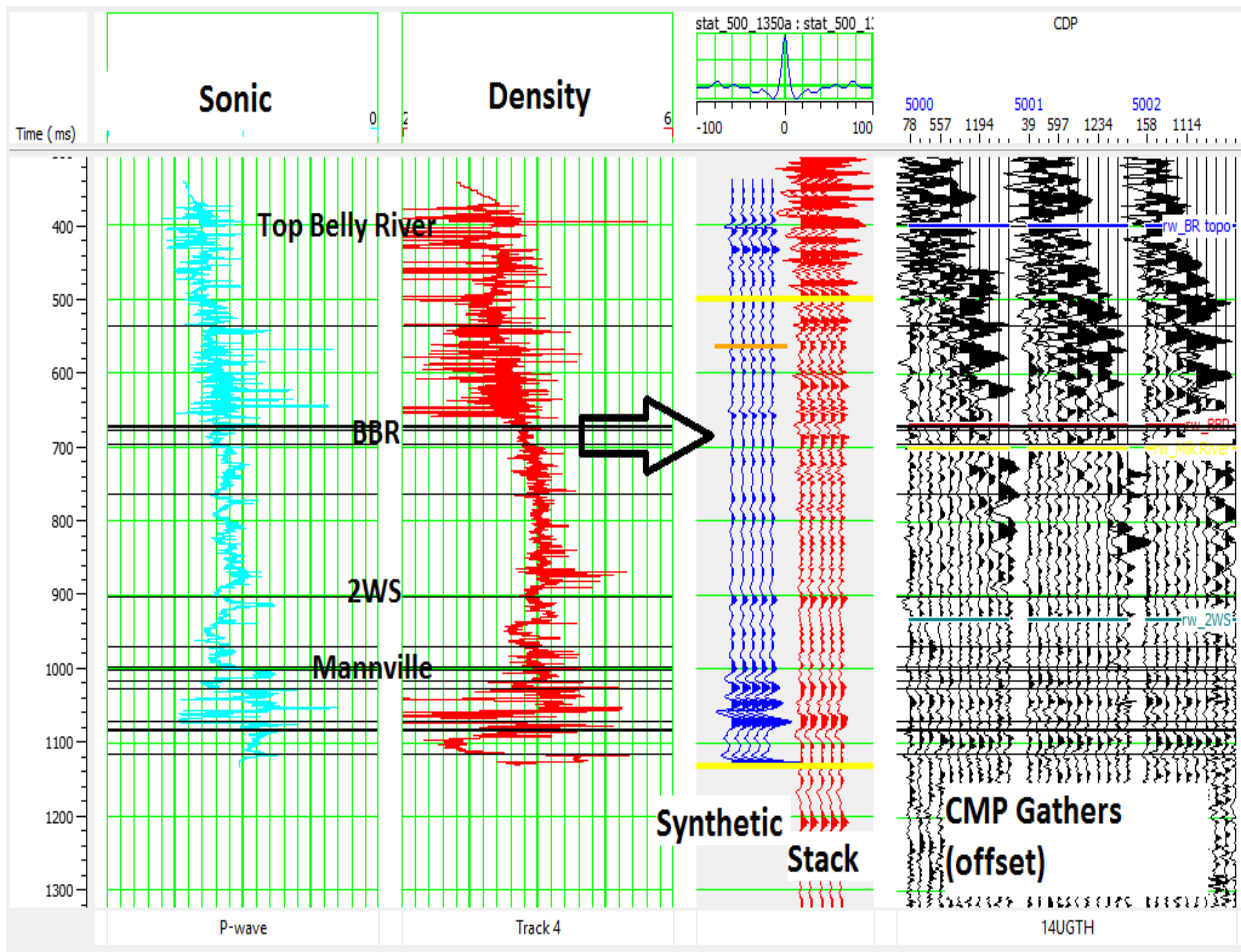


FIG 19, Seismic to Well Correlation, Geoview (HRS). This is a Geoview display of the seismic correlation from 03-18-34-22W4. There are CDP gathers included in this display. These same correlations are displayed in the Seisware synthetic correlation. The outside displays are the AVO forward model from 0 to 30 degree offset. The CMP trace display are the traces around the 04-12 well tie.

Data correlation from synthetic to actual is identical to that done in Seisware in the first part of this report, with the exception being a statistical wavelet derived from the

data was used for correlation. The synthetic trace, the stacked data and the prestack data were displayed simultaneously (Figure 19.) to insure the correlation was correct. Vista was used to run an F-X filter to reduce the random noise, super gathers were also run on both the F-X and the unfiltered stacks. This is shown on figure 15. The super gathers did an adequate job in reducing noise, The F-X version was not used because of possible harm to the signal.

Chung and Lawton (1980) presented a method of displaying a small number of CDPs as a gather to reduce noise and directly observe AVO behavior on CDP data. The super gathers on the unfiltered data set gave the best result for interpretation. (These gathers were often called “Ostrander Gathers,” after Neil Ostrander.) This technique allowed the subjective analysis of all the CMPs, and was very effective in random noise reduction. Coherent noise was an issue, F-K filtering was an option, however with 6-fold data, the effect was to attack the signal as well. If the data was higher fold, the F-X and F-K process would be more effective. The comparison of the Super Gathers to the well results are discussed in figures 26 to 31.

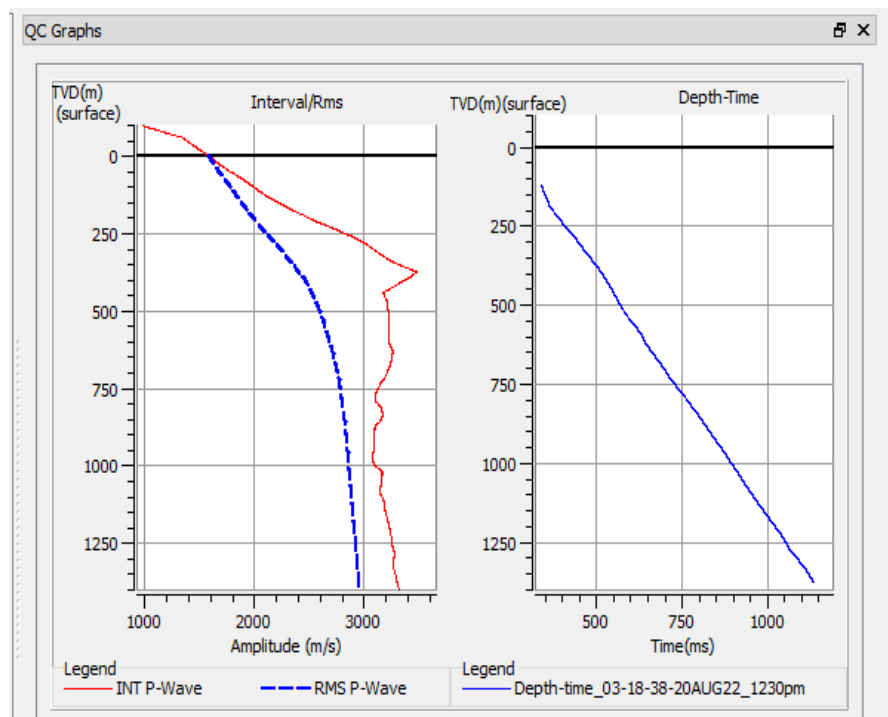


FIG 20. Time depth curve generated from 03-12 well tie

Before prestack inversion was available, supergathers were often used as a way to interpret AVO data. Other techniques were range limited stacks, and colour gradient analysis. Figure 22 shows a side by side comparison of the AVO forward gas model to a set of gathers near the 04-12 location. The simple stack is a very powerful method in reducing the signal to noise data, in much the same way as a CMP stack reduces multiples and coherent noise. The supergather preserves amplitudes, in that no process

is actually applied to the seismic data. F-X and F-K can attack signal, if the noise is similar in frequency or in phase with the signal.

With the time to depth relation established (Figure 20) the gathers were sorted into common incidence gathers. Figure 21 shows the common offset and common incidence gathers for line 14. Angle gathers are rearranged from offset gathers, based on the angle of incidence. Fatti's equation (figure 24) is expressed in angle of incidence rather than incident angle. Figure 21 illustrates the offset resorted to incident angle, with the 30-degree limit highlighted.

Figure 22 shows the AVO (in degrees) forward model on either side of CDP gathers sorted to the same range of angles. The time to depth relation was determined using the full synthetic. This shows the detailed correlation at the BBR zone, model with gathers.

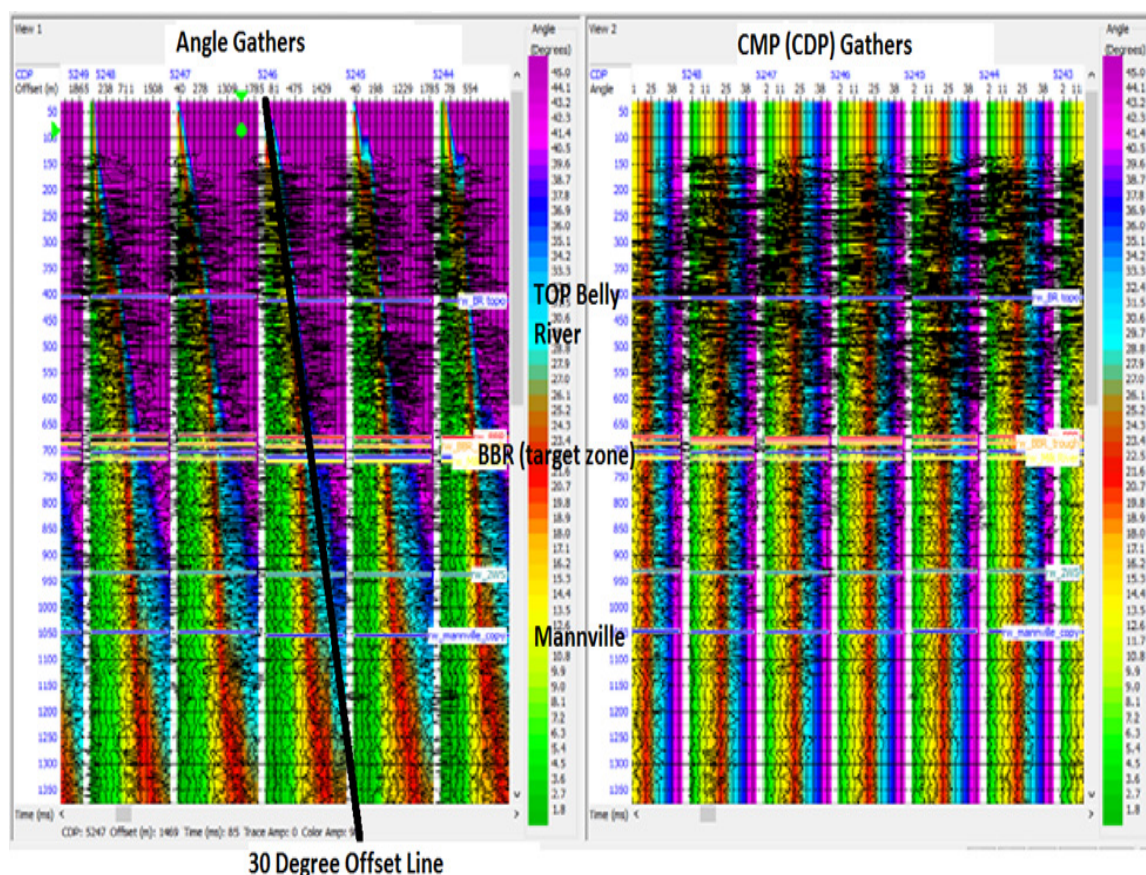


FIG 21. CDP and Angle gathers. These were calculated from the 04-12-38-22 well tie. Line 14 had a maximum useable offset of 30 degrees at the Basal Belly River. The fold was limited to 600 %, due to the acquisition parameters.

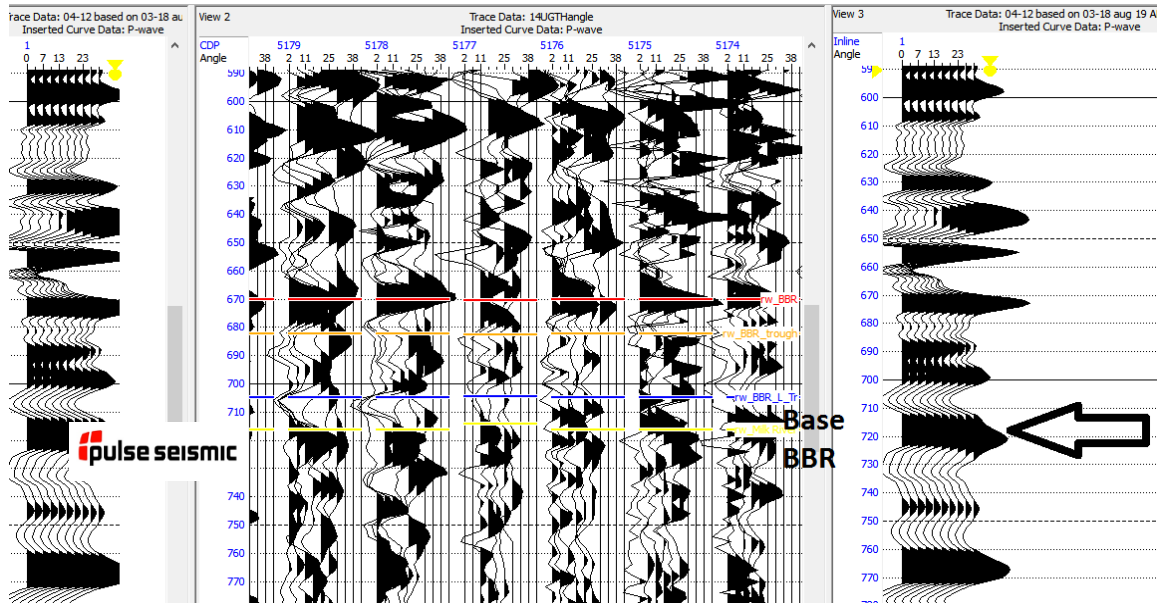


FIG 22. AVO model with CMP gathers at 04-12 location. This shows a general comparison of the AVO forward model to the CDP gather

PRESTACK INVERSION

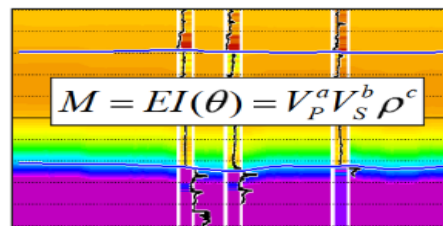
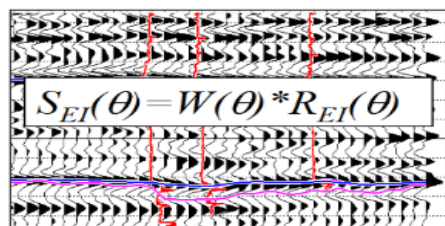
A poststack seismic inversion was processed on line 14. The results for the poststack were similar to those derived from the conventional seismic interpretation. The poststack inversion was used to set up the parameters for the pre stack simultaneous inversion. This sets up the time to depth correlation, the zone of interest, and the extracted wavelet.

This inversion used here is simultaneous, solving for V_p , V_s , and density. The pre stack gathers have horizons picked which constrains the inversion. The picks were straight lined into the offset domain, the noise on the data made the picks impossible using the auto picker. Where the signal to noise ratio was good, the inversion yielded believable results. Where the F-K noise became a problem, the quality of the pre stack inversion deteriorated.

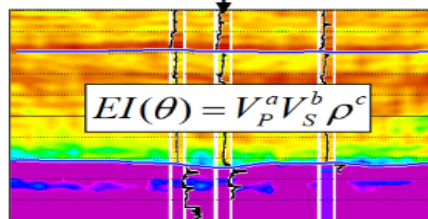
Elastic impedance inversion

HAMPSON-RUSSELL
A CGGVeritas Company

- (1) Optimally process the seismic data (2) Build model from picks and impedances



- (3) Iteratively update model until output synthetic matches original seismic data.



In elastic impedance inversion the seismic, model and output are as shown here.

FIG 23. Pre Stack Inversion Process. The pre stack inversion is a simultaneous process, it iteratively updates the model until the synthetic traces match the original seismic data. The higher the fold, and the lower the noise, the better the result. Line 14 was limited to 6 fold at the zone of interest, and had significant noise toward the west end of the line.

To run a prestack inversion, the model used for poststack inversion is the starting point (Russell 2005). The basis of the inversion is the normalized Fatti equation, which is determined as a function of the incident angle, not the offset.

AVO Simultaneous Inversion Theory

We start with Fatti's version of the Aki-Richards equation. This models the reflection amplitude as a function of incident angle; the weighted sum of Sonic, shear, and density. (figure 24.). Since Fatti's equation determines seismic reflectivity as a function of angle, in this case we are interested in the seismic data where the P-wave velocity decreases, the density decreases, and the S wave remains constant. This is another way of saying the Poisson Ratio diminishes. We have defined the zero offset reflectivity; the program indirectly delivers the S wave reflectivity by determining the S impedance as a function of the incident angle

Knowing the P, S, and density impedance values, Poisson Ratio, Lambda Rho, Mu Rho, Vp/Vs, Young's modulus can be calculated. Coal, with a high reflectivity will also generate a bright spot, however the AVO effect is a decrease in amplitude with offset. (Weir, Russell 1988). In this case we are looking for a low Poisson ratio, a low density, and a high shear wave velocity. This equates to a strong amplitude anomaly with in increase in AVO, or what is called a class III AVO anomaly (Spindler 2012).

We start with Fatti's version of the Aki-Richards' equation. This models reflection amplitude as a function of incident angle:

$$R_{PP}(\theta) = c_1 R_P + c_2 R_S + c_3 R_D$$

where:

$c_1 = 1 + \tan^2 \theta$ $c_2 = -8\gamma^2 \sin^2 \theta$ $c_3 = -\frac{1}{2} \tan^2 \theta + 2\gamma^2 \sin^2 \theta$ $\gamma = \frac{V_s}{V_p}$	$R_P = \frac{1}{2} \left[\frac{\Delta V_P}{V_P} + \frac{\Delta \rho}{\rho} \right]$ $R_S = \frac{1}{2} \left[\frac{\Delta V_S}{V_S} + \frac{\Delta \rho}{\rho} \right]$ $R_D = \frac{\Delta \rho}{\rho}$
--	--

FIG 24. Fatti's Equation. This expresses the Rpp (p-wave reflectivity) as a function of incident angle. (Weir, Russell 2016)

Normalised Equation

This changes Fatti's equation to:

$$R(\theta) = \tilde{c}_1 W(\theta) D L_P + \tilde{c}_2 W(\theta) D \Delta L_S + c_3 W(\theta) D \Delta L_D$$

where:

$$\tilde{c}_1 = (1/2)c_1 + (1/2)kc_2 + mc_3$$

$$\tilde{c}_2 = (1/2)c_2$$

$$W(\theta) = \text{wavelet at angle } \theta$$

$$D = \text{Derivative operator}$$

$$L_P = \ln(Z_P)$$

Figure 25. Normalized equation. (Weir, Russell 2016)

Relationship of Variables

We want to use the fact that the basic variables, Z_p , Z_s , and ρ are related.

We start with two relationships which should hold for the background “wet” trend:

$$\begin{aligned} V_s / V_p &= \gamma = \text{constant} \\ \rightarrow \ln(Z_s) &= \ln(Z_p) + \ln(\gamma) \end{aligned}$$

Constant γ

and:

$$\begin{aligned} \rho &= aV_p^b \\ \rightarrow \ln(\rho) &= \frac{b}{1+b} \ln(Z_p) + \frac{\ln(a)}{1+b} \end{aligned}$$

Generalized
Gardner

FIG 27. Variable constraints The model is generated by the user, sonic density and shear wave logs are tied to the seismic data. Seismic events (horizons) are correlated on the stack data. A wavelet is extracted to apply to the seismic data to ensure the data is zero phase. The model accounts for the low frequency (0 to 15 Hz) component by blocking the logs in time, constrained by the user using a series of horizon picks. This part of the process is identical for pre and poststack inversion. . (Weir, Russell 2016)

Model constraints

Both these relationships lead us to the more general model for the background trend:

$$\ln(Z_S) = k \ln(Z_P) + k_c + \Delta L_S$$

$$\ln(\rho) = m \ln(Z_P) + m_c + \Delta L_D$$

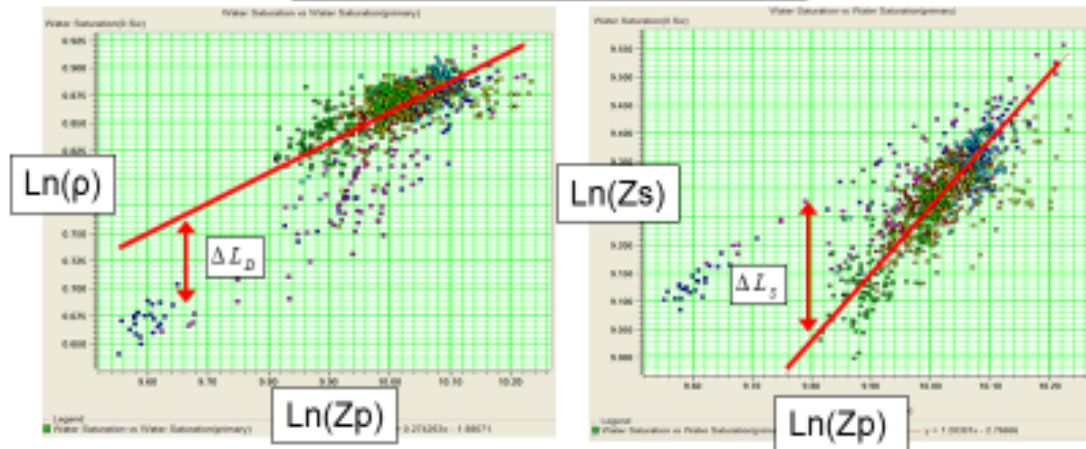


FIG 28. Model constraints, Log -Log constraints. (Weir Russell 2016)

The model is defined by the user, sonic density and shear wave logs are tied to the seismic data. Seismic events (horizons) are correlated on the stack data. A wavelet is extracted to apply to the seismic data to ensure the data is zero phase. The model accounts for the low frequency component. In addition the inversion is constrained by interpreted seismic boundaries. The model is perturbed a number of times until a best fit is found with the prestack seismic data. This process is stable in that V_p/V_s ratio is constrained to a limited range of values. There are also limits to how far density and sonic can deviate. The inversion could become quite unstable without the constraints, Poisson's ratio could become negative, and the density could become 0 or quite large in order to match the offset traces.

SIMULTANEOUS INVERSION RESULTS

The inversion worked well where the data had a high signal to noise ratio, but became difficult to interpret in the noisy areas. A five trace CMP mix was applied to the data to help mix the random noise. The choice of colour used to highlight the desired attribute in the seismic data. For each well location, displays of the simultaneous inversion were displayed along with the CMP gathers. At the 04-12 gas well, there is a significant AVO and amplitude effect, the inversion had difficulty in

modeling a solution through the F K noise. Figures 31 to 36 display the inversion results, the angle gathers, at the specific well tie locations.

DISCUSSION AND ANALYSIS

The AVO was analyzed over several well ties, and are shown with their position on map view, and the Gather and inversion response. The ties were picked to show the off channel response, the gas response, and back to the off channel response across the mapped pool boundary. These well ties show the super gather response as well as the Z_p (elastic p-wave) inversion.

There were several well ties available to compare the results of the seismic evaluation. The wells ranged from 8 meters pay, to tight, non porous BBR. The data quality varied, coherent F-K noise became a factor near the 04-12 well tie. The 5 CDP mix supergather appeared to be the most stable way to deal with the noise problem. The gathers generated a seismic signature that could be qualitatively interpreted along the line. Running the F-X deconvolution showed a marked improvement in the overall quality of the unstacked CDP gathers. When the gathers, raw and F-X were stacked into supergathers, the raw supergathers appear to give better results. It is likely that the main contributor to noise was coherent F-K noise. The option for running a pre stack F-K was available, however F-K can attenuate AVO effects.

The use of summed CMP gathers is sometimes referred to as “Ostrander” gathers. Chung and Lawton (1980) used a similar technique to Image a Glauconitic Gas sand bar. The summing of 6 adjoining CMP gathers into common offsets did a very good job in reducing random noise. Here, the same technique is deployed, but the displayed gathers are a running average of 5 CMPs. The visualization software allows the user to scroll across the entire data set, identifying prospective areas. The advantage of this gather summing technique over F-X prediction or F-K filtering is there is no of AVO attenuation only averaging.

The wells were within 300 meters or less of the seismic line, there were offline effects observed at the intersection of line 14 and 16. 2-D seismic data can be subject to off line effects, and such appears to be the case with the 09-06 well tie. Line 14 and line 16 crossed an amplitude feature giving conflicting amplitude results. Line 14 had a strong anomaly, line 16 did not. The termination of the anomaly occurred near the intersection. This strongly suggests contributions of off line seismic effects. This apparent contradiction in amplitude anomalies exemplifies the risk associated with drilling seismic features on 2-D data, particularly in a rapidly changing depositional environment.

Displays of the pre stack inversion as well as the super gathers were displayed at each of the well locations. An undrilled amplitude anomaly was also displayed to demonstrate how AVO analysis could be used to highlight seismic features. This analysis ties several well ties, and is the process to evaluate what the data is saying at each data point. The supergathers appear to be the most stable and informative way to

deal with the noise. The inversion works well, with good data; It tends to fall apart in noisy areas.

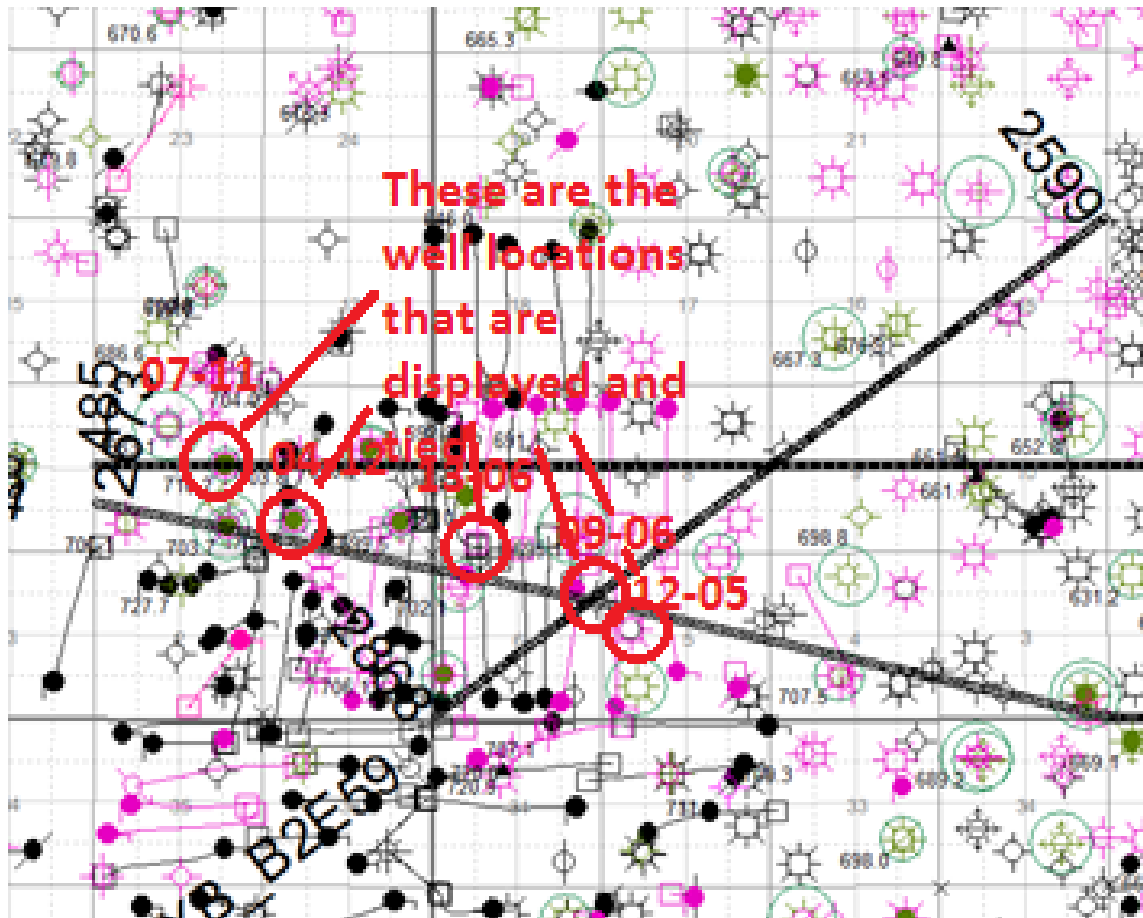


FIG30. Index map for well ties The following figures are the well ties from West to East.

The Yellow event, (Lea Park / Bottom of the BBR pay) marked with an arrow in all of the following figures marks the base of the gas pay. The expected gas response is a strong amplitude trough above the event, and the Yellow peak will also be strong. The Yellow event was picked on the stack section and interpolated into the gathers. There are stratigraphic changes within the BBR, so the amplitude event will move up and down a few milliseconds in response to different pay heights.

At the West end of the line is the tie to 07-11 (figure 31). This location was mapped as the west boundary of the pool. This location is 400 meters North of the seismic line, so the well tie shown is based on an estimate of the geological trend. At the BBR zone of interest, the amplitude response is weak, and there is minimal amplitude and AVO effect. The inversion shows no direct indication of gas sand, confirming the anticipated response from a tight regional sand. The amplitude response gets stronger to the East of the well tie, consistent with the Geological mapping.

The 04-12 location is approximately 150 meters offline (figure 32). The inversion is not conclusive; however, the gathers show an AVO effect, as well as a strong amplitude response. F-K noise was a problem with the data at this location, this coherent noise is also evident on the inversion. The 04-12 location has 7 meters of gas pay on trend with the seismic line. The AVO anomaly rises in structure a few CDPs to the West. This movement over a limited time range is expended in an estuarine environment.

The 13-06 location has three meters of gas pay and sits approximately 300 meters off line. It is located in the mapped belly river trend. Figure 29 also shows the well location and its projected position on the seismic line. Noise is less of a problem here, so the low impedance (yellow) is in general agreement with the geological trend, thickening to the west.

09-06 is a direct well tie at the intersection of line 14 and line 16 (figure 34). The well logs identify the facies as tight, at this location. The amplitude on line 14 suggest and anomaly, as well as the AVO response. There is a mistie in the amplitude response between line 14 and line 16 (figure 17), however all other events tie quite well. This suggests that line 14 is imaging something close to, but off of the seismic line. The gathers get weak 5 CDPs to the west. If this were part of a 3-D survey, the anomaly would be located much more accurately.

12-05 marks the East boundary of the mapped seismic BBR pool (figure 35). The response is consistent with the modeling, both in stacked amplitudes and AVO response. To the East of this location there is a strong amplitude anomaly (figure 36). If one was to rely solely on the zero offset modeling, the amplitude would be considered a BBR prospect. Other effects can happen to create strong amplitude events on seismic, the most common being coal. This amplitude anomaly can be discounted because, although the stack amplitude response is strong, the AVO response is weak. The amplitude appears to originate below the base of the BBR gas zone, and may be an upper side lobe of an event occurring below the BBR.

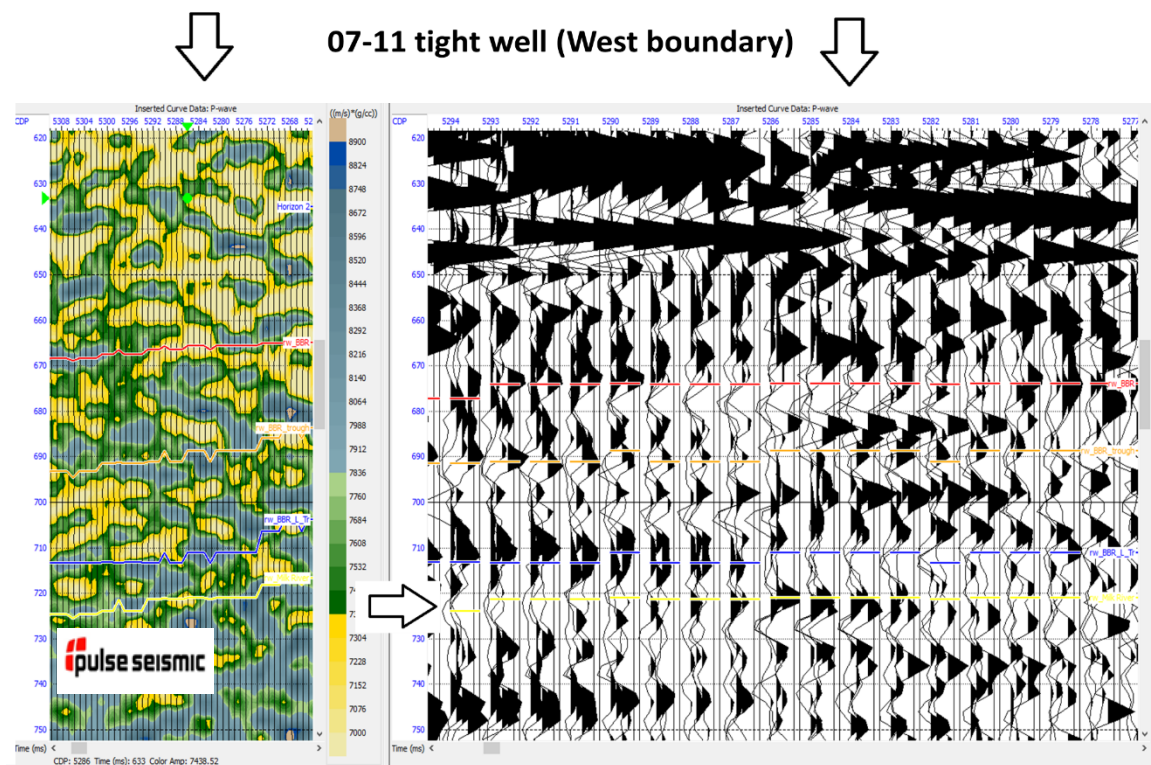


FIG 31. 07-11-038-22W4. The 07-11 well is located on the East boundary of the mapped BBR pool. The AVO response is flat or decreasing, the amplitude is weak, and the inversion indicates a tight facies.



FIG 31a. Well tie position, 07-11-038-22W4

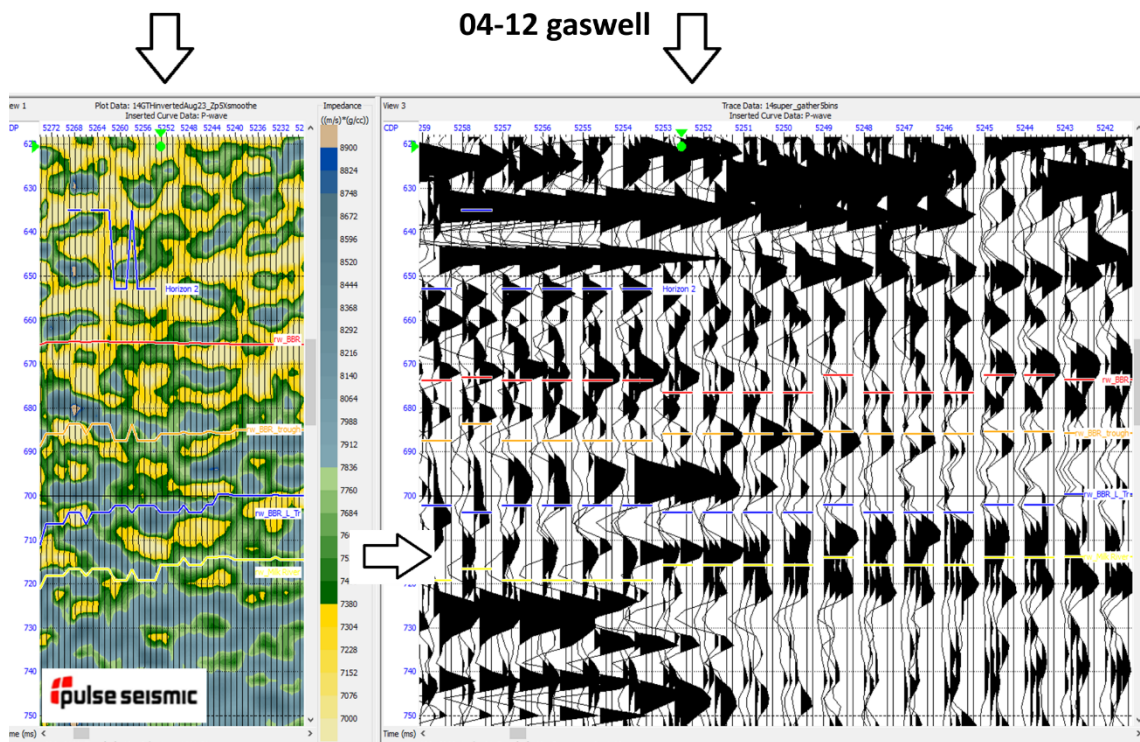


FIG 32. 100/04-12-038-22W4, CDP 5254, SP 2627. The location is projected into the line from 150 meters north. The arrows show the projection of the well bore and the target zone. The CMP super gathers show a strong increase in AVO, the Zp inversion shows a weak low impedance anomaly. This is the thickest BBR gas well in the area, 7 to 8 metres of pay. This is a strong direct correlation between AVO effect and gas pay.

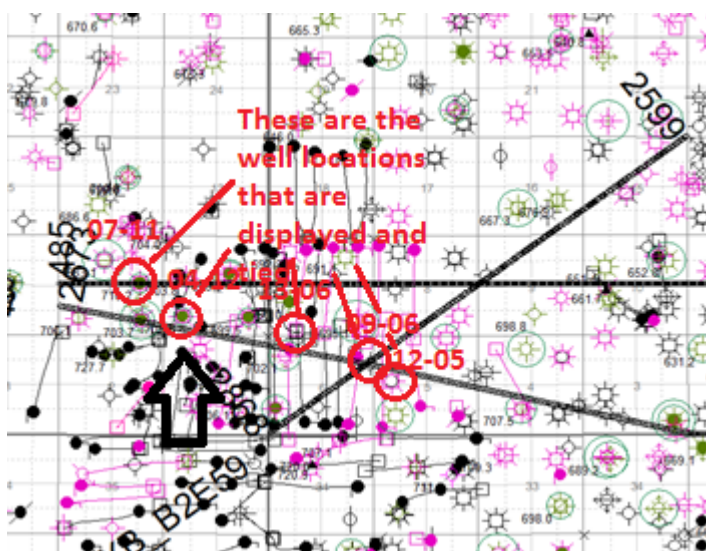


FIG 32a. 100/04-12-038-22W4 location

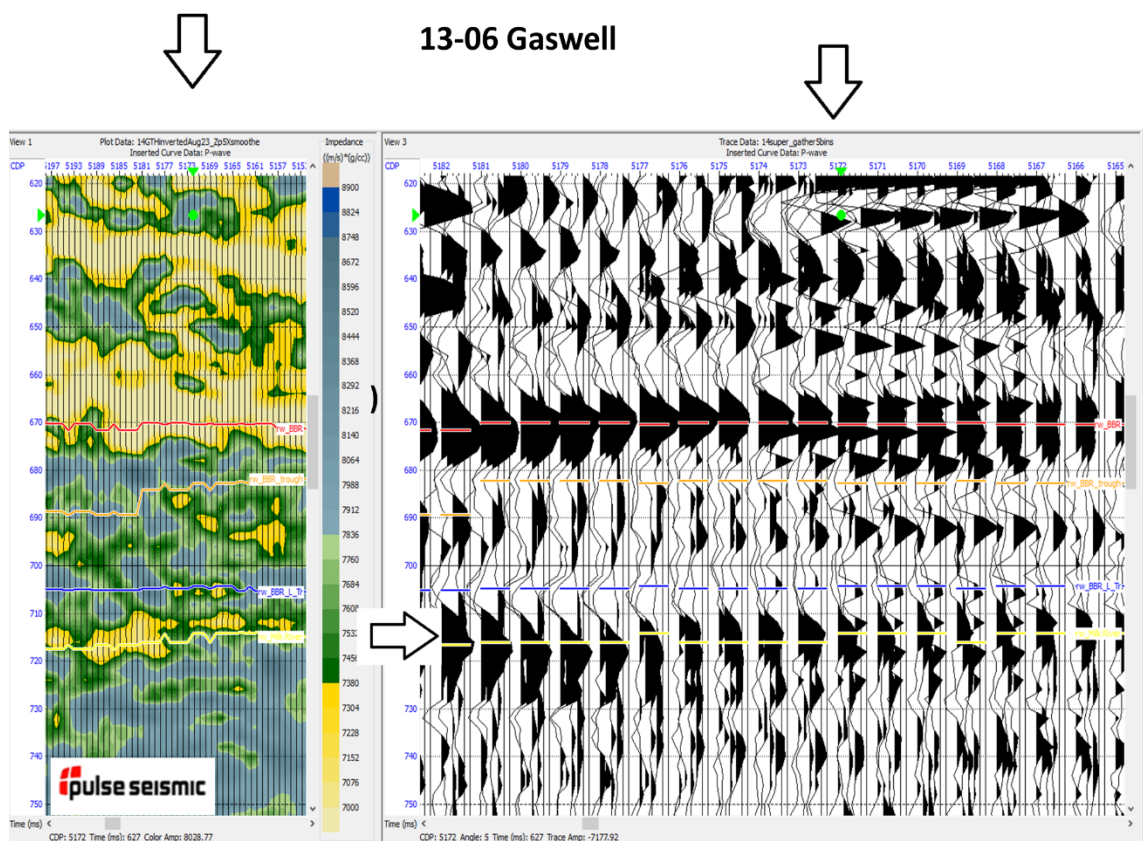
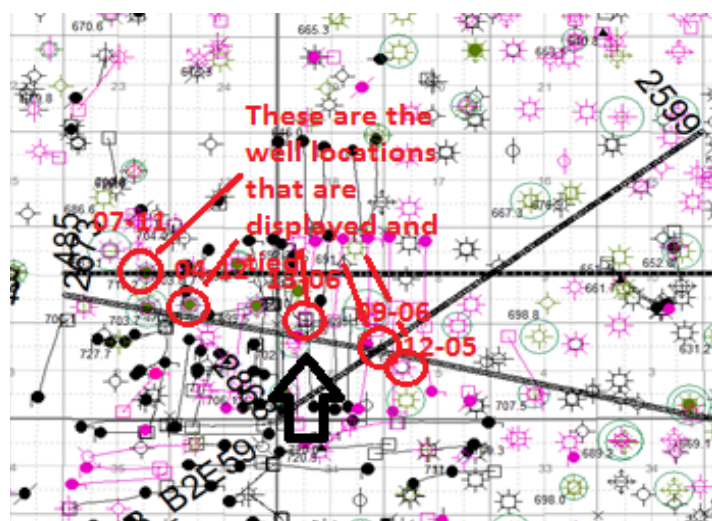


Fig 33. Inversion and AVO gathers at 13-06-34-21W4 CDP 5164. This lines ties the well approximately 250 meters to the North West, giving some ambiguity as to where the well actually ties. Geological mapping indicates the pool thickens to the West, the gathers and inversion also indicate a thickening of pay to the West. The yellow patch would indicate a thick, low impedance zone at CDP 5182



33a. Well Tie Position 13-06

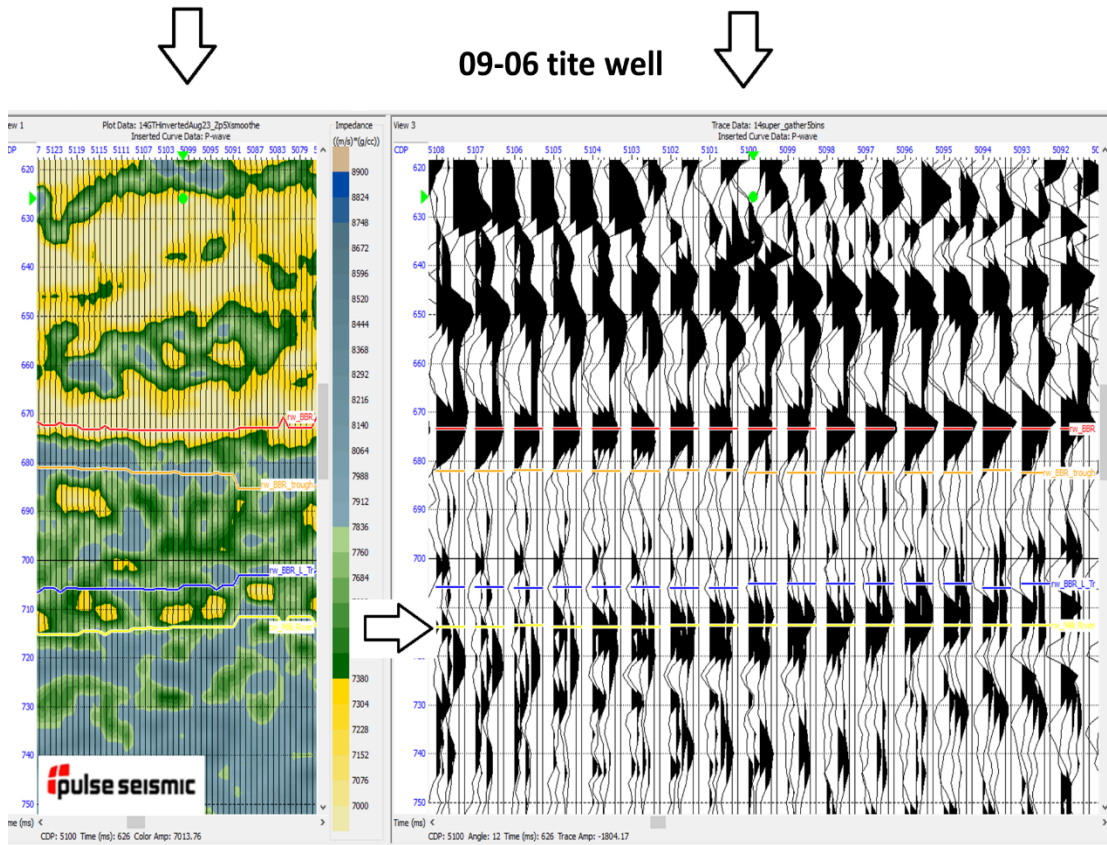


FIG 34. 100/09-06-038-21W4, CDP 5100, SP 2550, line 16 CDP 5100 At the 09-06 location the BBR is tight. The supergathers indicate a small positive anomaly. There is an intersecting line 16 that has a weak seismic amplitude. The seismic amplitude misties for the two lines suggesting that the actual anomaly may be off line (Fresnel Zone effect)



FIG 34a. 09-06 location. This is located at the intersection of lines 14 and 16

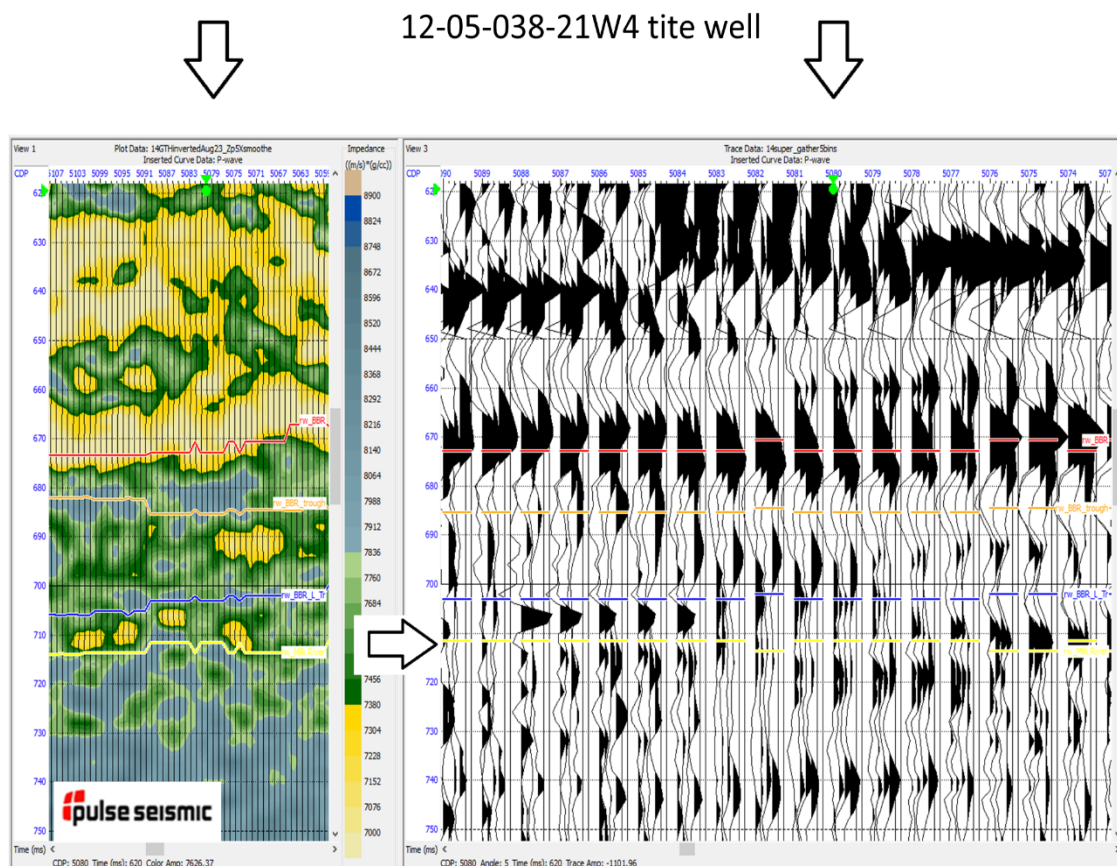


FIG 35. 100/12-05-038-21W4, CDP 5080, SP 2540. 12-05 is in the tight reservoir facies. The supergathers show a weak amplitude and a flat AVO response. The inversion shows a lower impedance. Given the model and the observed response, the response is consistent with tight sand.

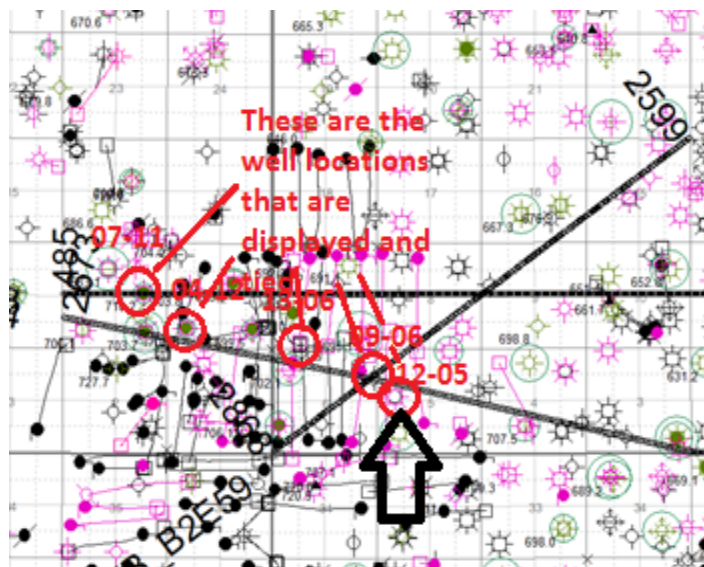


FIG 35a. 100/12-05-038-21W4. The BBR at 12-05 is tight.

Undrilled amplitude anomaly

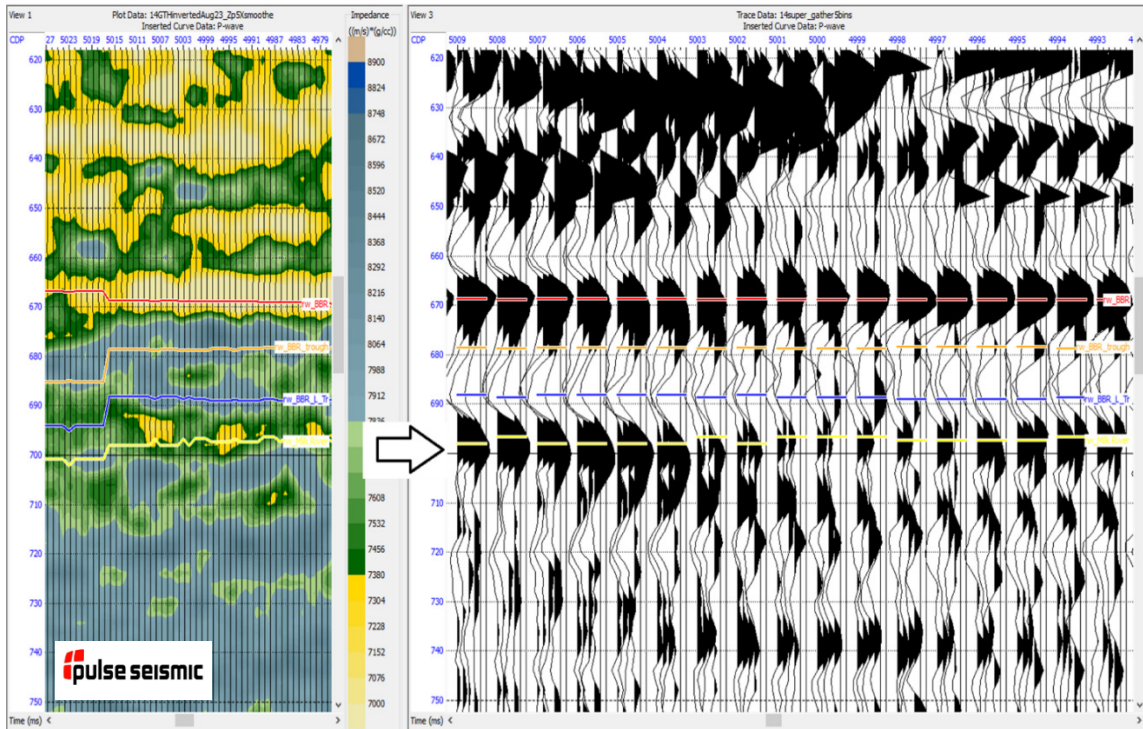


FIG 36. Undrilled amplitude anomaly without AVO effect. The stacked amplitude is strong, the AVO effect indicates tight sand. Often features like these are considered 'bright spots.' This anomaly is caused by effects other than gas. It appears to originate below the base of the BBR.

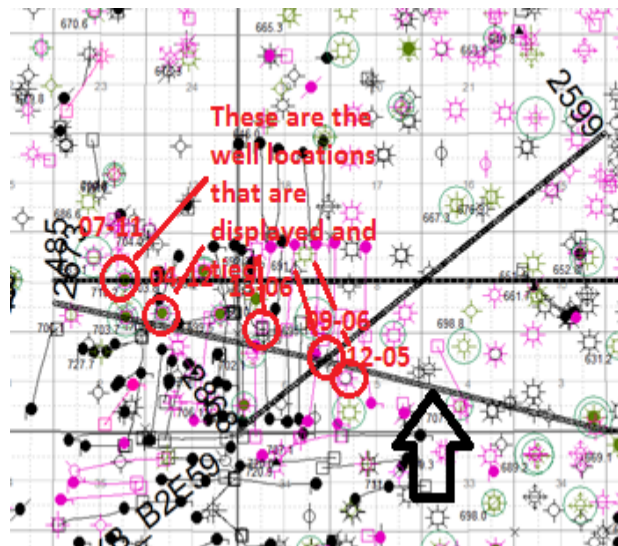


FIG 36a. Location of Amplitude Anomaly

CONCLUSIONS AND RECOMMENDATIONS

Given the depth and pay thickness, the Basal Belly River Gas is a viable seismic target. Vintage 2-D Seismic data can be used for direct detection of Hydrocarbon reservoirs. As with 2-D interpretation, AVO analysis on 2-D data faces the same challenges as conventional interpretations. Images may come from off line effects (Fresnel zone), as seen in the area where line 14 and line 16 intersect. Lack of usable fold over the zone of interest contribute to some of the ambiguous results obtained from the prestack inversion.

Higher fold 2-D data, as well as 3-D data would yield more accurate data in the mapping and direct detection of Belly River Gas. Higher fold would be required to get a more stable pre stack response. 3-D data would be an improvement as well, off line effects would be far less of an issue. FK noise created high amplitude events that made it difficult for the inversion to get a good image. The pre stack supergathers provided a method to subjectively evaluate gas pools, effectively allowing the interpreter to see *through* the noise.

This methodology employed in Rangeland can be extended to areas where the intent is to evaluate Basal Belly River Gas. Higher fold 2-D, and 3-D data would address the issues of noise, both coherent and random. 2-D data would be a valuable tool in a reconnaissance role to evaluate prospective sections.

As an exploration strategy, geological mapping has given potential areas. The vintage 2-D seismic can be reprocessed and used for detection of specific parcels of land on a reconnaissance basis. The AVO processed supergathers appear to be a good way to identify potential targets. After the land has been acquired, new seismic needs to be acquired to identify drilling locations. The data needs to be 3-D or 2-D data with a minimum of 12 – to 20 fold at the zone of interest.

With higher fold data, more accurate estimates of pay thickness and reservoir quality can be achieved. 3-D data would give a more exact location, given the complexity of the estuarine depositional system. Prestack inversion would provide a very accurate reservoir description in the BBR target for the Rangeland area.



REFERENCES

- Alberta Geological Survey, Geological map, Accessed online, July 2016. <http://geology.about.com/library/bl/maps/blalertamap.htm>
- Bancroft, John, A Practical Understand of Pre- and Poststack Migrations, Volume 1, January 2016. University of Calgary.
- Boulder Operations, Belly River Stacked Sands Brazeau Property Review, 2016
<http://www.boulderenergy.ca/Operations/Brazeau-Property-Overview/Belly-River-Stacked-Sands/index.php>
- Chung, Hai-Man, Lawton, Don AVO Analysis and Complex Attributes for a Glauconitic Gas Sand Bar Canadian Journal of Exploration Geophysics VOL. 26, NOS 1 B 2 December ,1990). Pi 72-86
- Choi, Kyung Sik, Dalrymple, Robert W., Chun, Seung Soo, Kim, Seong-Pil , Sedimentology of Modern, Inclined Heterolithic Stratification (IHS) in the Macrotidal Han River Delta, Korea, Journal of Sedimentary Research 2004.
- Crain, Ross, Crain's Petrophysical Handbook, published online, January 2000, Accessed April 06 2016 <https://www.spec2000.net/25-edit15.htm>
- Hampson, Dan, Russell, Brian, Hampson-Russell Software Bankhead, Brian, VeritasDGC. Simultaneous inversion of pre-stack seismic data, 2005 CSEG Convention.
- Irwin, Kenneth, Depositional Environments and Diagenesis of the Basal Belly River Sand, Strathmore area, Alberta Canada. 1980 M.Sc. thesis. Texas Tech University
- Isaac, J. Helen and Lawton, Don C. CREWES, University of Calgary. A case study of an offset – dependant synthetic seismogram, GeoConvention 2016, Calgary Albert
- Kyungsik Choi, Faculty of Earth Systems and Environmental Sciences, Chonnam National University Tidal and seasonal controls on the morphodynamics of macrotidal Sukmo Channel in Gyeonggi Bay, west coast of Korea –implication to the architectural development of inclined heterolithic stratification
- Lawton, Don, CMC (CaMI) information PD
http://conference.co2geonet.com/media/1129/cami-ccs-field-research-station_lawton-et-al_cmc-research.pdf
- Millar John, and Bancroft, John C, Multigrid deconvolution of seismic data, CREWES Research Report Volume 16 (2004)

Russell, Brian 1 Hampson-Russell Software2010. Making sense of all that AVO and inversion stuff! The Milton Dobrin Lecture, April 2000.
Spindler, P, Rengifo, R. Coulon, D., Lenoir, N., Ariawan, S. Rengifo R., It Is Never Too Late for Seismic, How Geophysics Contributed to Rejuvenating a Mature Field, Tunu Shallow Gas Development. Search and Discovery Article #20173(2012) *Posted September 2012
Weir, Ronald; Russell, Brian 1988 CSEG presentation, Amplitude Vs. Offset analysis, the Kiskatinaw and the Colony, a Comparative Case study. 1988 CSEG convention.
Wikipedia, Belly River Group, accessed online August 2016.
https://en.wikipedia.org/wiki/Belly_River_Group

TECHNICAL SOFTWARE USED

Geoview (HRS), pre and poststack inversion
Geosyn, 2-d modeling and petrophysics
Geoscout, Well grid and culture data base, LAS files, production and perforation information
Seisware, Conventional seismic interpretation
Vista, prestack data preparation.

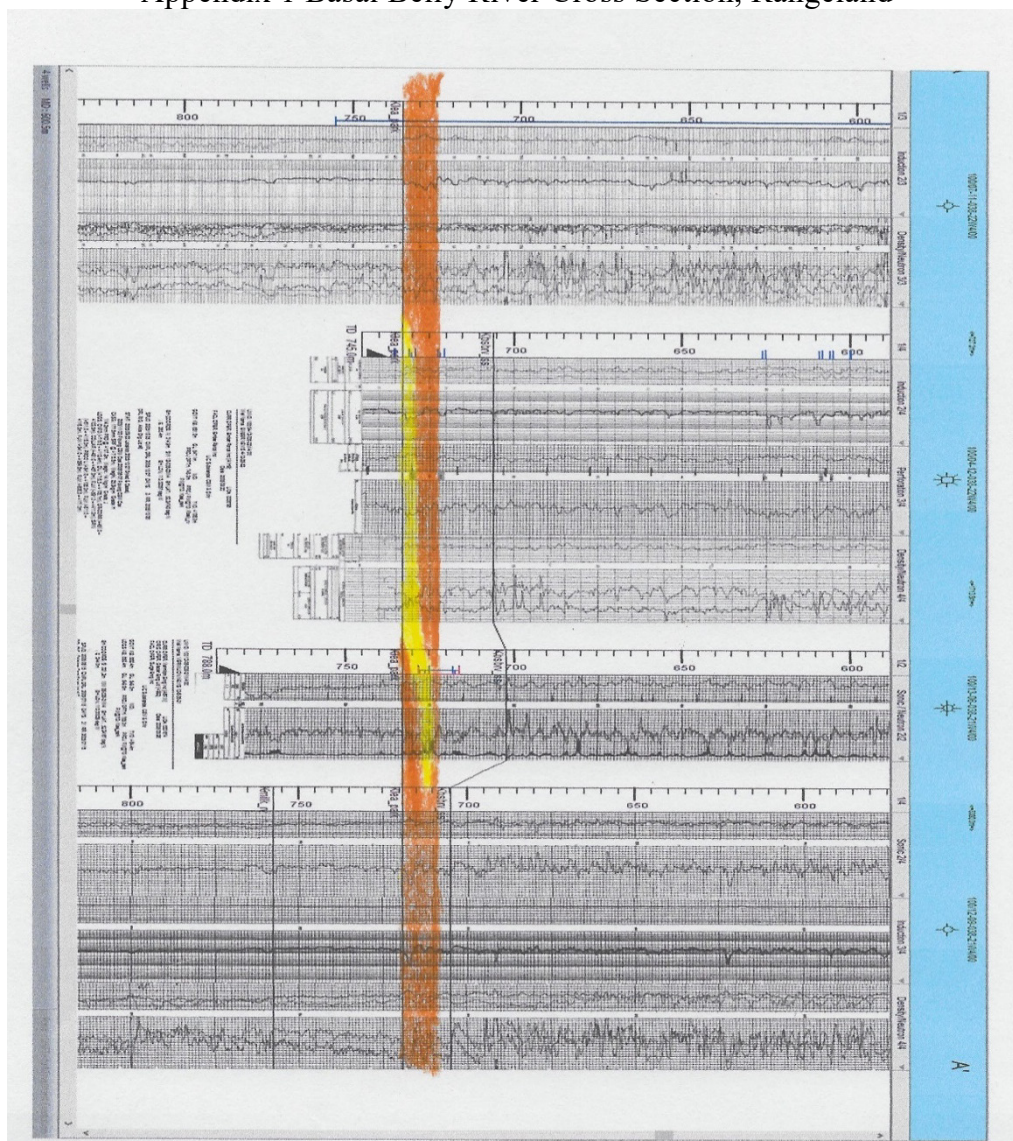
CONTRIBUTORS

Statcom, access to their reprocessing facilities, Peter Snethledge, Tor Hagland
Pulse data, Proprietary data provided as a contribution to the University of Calgary
Dr. Brian Russell, technical advice and consultations
Dr. R Meyer, advice on petrophysics and log calibration

ACKNOWLEDGEMENTS

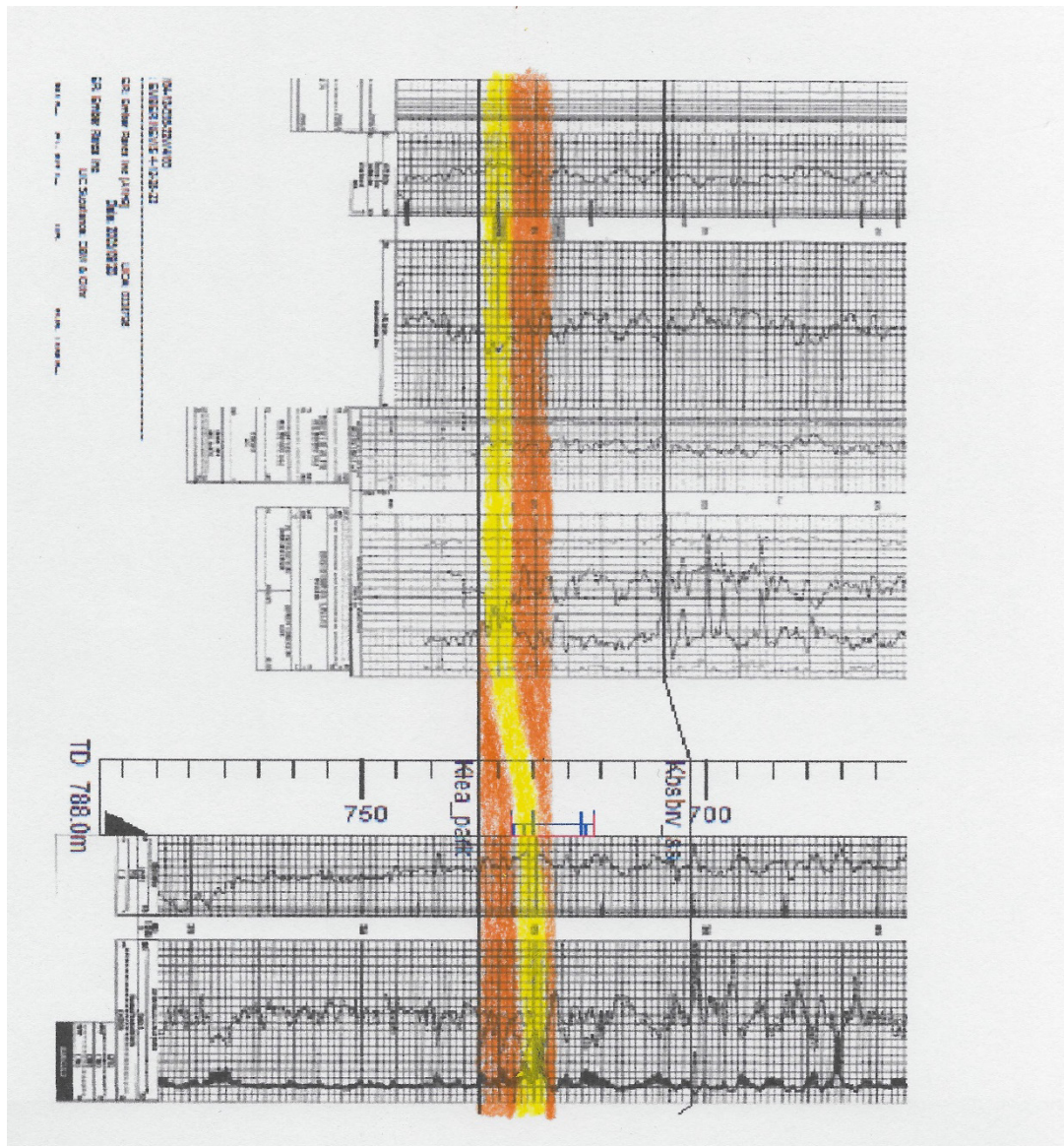
We thank the sponsors of CREWES for continued support. This work was funded by CREWES industrial sponsors and NSERC (Natural Science and Engineering Research Council of Canada) through the grant CRDPJ 461179-13.

Appendix 1 Basal Belly River Cross Section, Rangeland



Appendix 1 Basal Belly River Cross Section, Rangeland. The gas pay zone is highlighted in yellow.

APPENDIX 1B.



Appendix 1b. Basal Belly River Cross Section, Rangeland. The gas pay zone is highlighted in yellow.